A STUDY OF POISSON'S RATIO IN THE UPPER CRUST OF THE SOCORRO, NEW MEXICO, AREA

by

Frank J. Caravella

Submitted in partial
fulfillment
of
the requirement
of
Geophysics 590
and the
Master's Degree Program
at
New Mexico Institute
of
Mining and Technology

December, 1976

Abstract

In order to find the average Poisson's ratio and spatial distribution of Poisson's ratio for the Socorro region, a twelve month survey of microearthquake activity in the vicinity of Socorro, N.M., was made using high gain (5.6 million at 60Hz) seismographs. Of the many events recorded during this time, 50 were selected on the basis of the number of recording stations and data quality. The 50 located microearthquakes in this study seem to be associated with three major structural features: (1) the area near or within Socorro Basin centered approximately 5 km north-northwest of Socorro, (2) the southwestern margin of Socorro Mountain, and (3) the southern end of the La Jencia Basin.

Wadati diagrams were drawn for each of the events to find the associated Poisson's ratio. The 50 Wadati diagrams indicated an average Poisson's ratio of 0.262 with a standard deviation of 0.034 for the Socorro area. This average Poisson's ratio is about 21 percent greater than the value of 0.217 found for crustal rock further north in the rift (Sakdejayont, 1974). The difference in Poisson's ratio implies a difference in Vs for the two areas, 3.30 km/sec versus 3.49 km/sec.

Initially, using a composite Wadati diagram or ray-path technique, three Poisson's ratio anomalies within

the upper crust were defined: one in the southern La Jencia Basin, a second just below Socorro Mountain, and a third in the central La Jencia Basin. The average Poisson's ratios assigned to these anomalies were 0.292, 0.289, and 0.284 respectively. However, taking into account the locations of the hypocenters used in defining the anomalies, it was found that only two anomalous areas could be supported by this study. One is located in the southern La Jencia Basin while the other is north of station CM.

Of the factors which affect Poisson's ratio, (1) fracturing (fluid or gas-filled), (2) pressure-temperature (assuming a normal geothermal gradient), and (3) composition, none could adequately explain the observed Poisson's ratio anomalies. However, one or more shallow partial melts could explain the anomalous Poisson's ratios.

The study of Poisson's ratio cannot be used at this time to make any geothermal resource estimates. But one area in the investigation of geothermal resources in which the study of Poisson's ratio might be useful is indicating those areas which could have magma present.

Introduction

The purpose of the study described in this report was (1) to find an average Poisson's ratio for the local Socorro region from 50 located microearthquakes and (2) to determine the spatial distribution of Poisson's ratio in the upper crust from body waves generated by the 50 microearthquakes. Of special interest in this study was the location of areas in the Socorro region with anomalously high Poisson's ratio because these segments of the crust may contain magma.

Data Collection

This study incorporated the use of five to six Sprengnether Instrument Company MEQ-800 portable seismographs. Each system consisted of either a Mark Products L4C (1.0Hz) or a Willmore (1.5Hz) vertical seismometer, a gain stable amplifier, a quartz-crystal controlled timing system, and a smoked paper helical recorder which operated at a recording speed of 120 millimeters/minute.

A magnification versus frequency plot is shown in Figure 1 for the MEQ-800 seismographs at the most typical gain and filter settings. Gain settings could be varied from 60 to 120 db (6 db steps), depending on the amount of background noise. Filtering of high and low frequencies was possible, but only signals above 30Hz were ever filtered.

Clocks on all seismographs were synchronized to WWV-UST at the onset of each recording period (4 days). The clocks were similarly checked for drift at the end of the recording period. Any drift of the clock was assumed to have occurred linearly and timing corrections were made accordingly.

This study uses 50 events which were recorded from May, 1975, to April, 1976. Many different arrays were used during this time period, and in all, 17 different

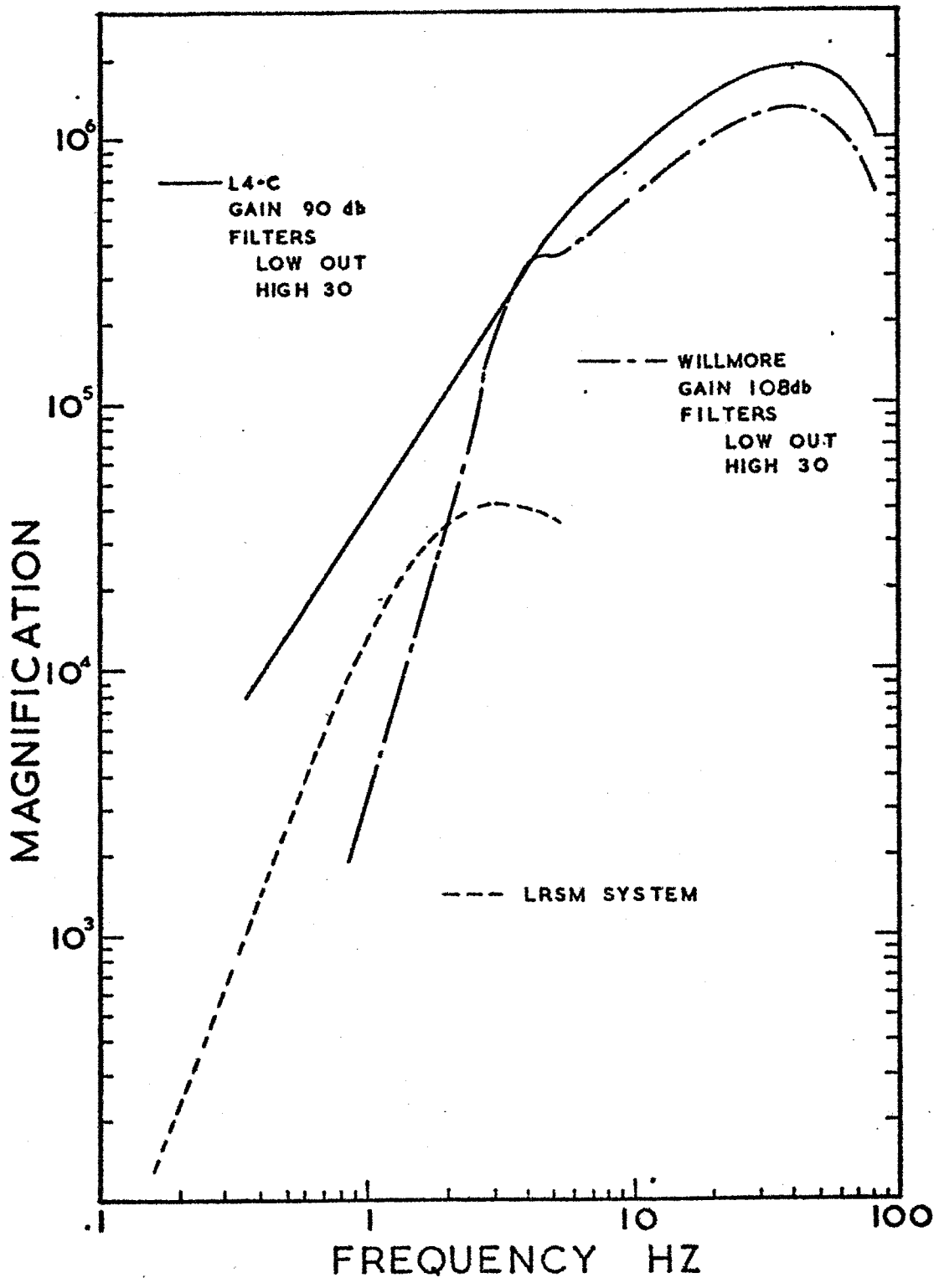

Figure 1. Magnification curves of MEQ-800 seismic unit with an L4C or Willmore geophone at the most typical field settings.

station locations were occupied (Figure 2). All stations were located on consolidated sediments or igneous rock in order to minimize arrival time delays. Station locations along with meanings of station letter designations are listed in Table 1.

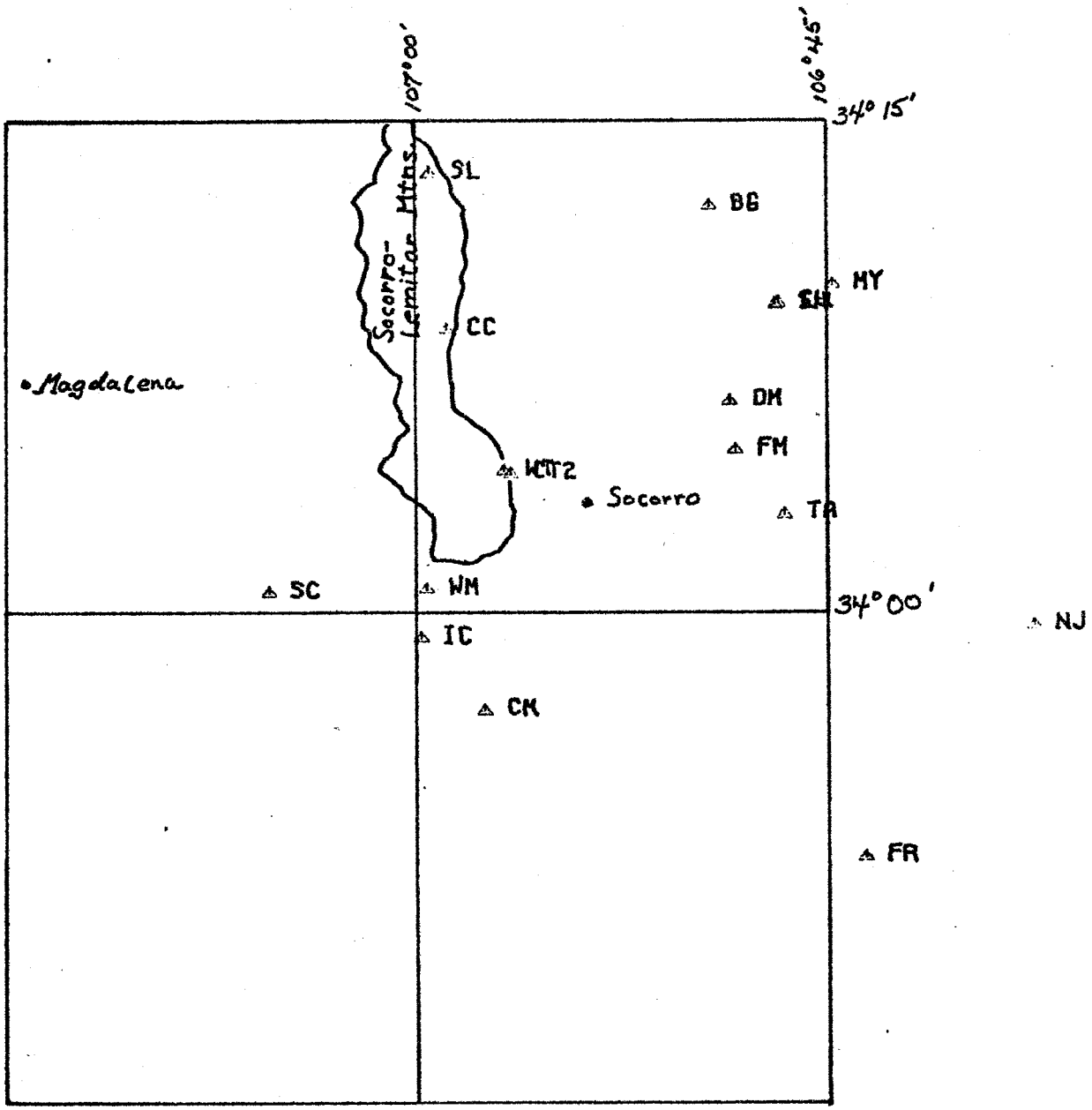

Figure 2. Seismic stations occupied in this study.

Table 1. The Meanings of Station Letter Designations and Locations of Seismic Stations Used in this Study.

STATION	SYMBOL	LATITUDE	LONGITUDE	ELEVATION
WOODS TUNNEL	WT	34.0722	106.9459	1555m
WINDMILL	WM	34.0120	106.9929	1673m
TAJO ARROYO	TA	34.0498	106.7751	1558m
STONE HOUSE	SH	34.1570	106.7802	1577m
SOUTH CANYON	SC	34.0100	107.0894	2073m
NORTH JOURNADA	NJ	33.9924	106.6253	1644m
MESA DEL YESO	MY	34.1667	106.7459	1645m
INDIAN CAVE	IC	33.9870	106.9967	1730m
FITE RANCH	FR	33.8747	106.7270	1558m
DUCHESS MINE	DM	34.1075	106.8079	1536m
CANONCITO DE LA UVA	CU	34.1573	106.7785	1585m
CHUPADERA MINE	CM	33.9501	106.9576	1640m
BOWLING GREEN	BG	34.2068	106.8205	1516m
CORKSCREW CANYON	CC	34.1442	106.9812	1649m
FLUORITE MINE	FM	34.0829	106.8047	1573m
SAN LORENZO	SL	34.2234	106.9910	1615m
CENTER TUNNEL 2	CT2	34.0707	106.9418	1510m

Location of Microearthquakes

Procedure

Two methods were used to locate the 50 events in this study: one involved the use of a computer-adapted graphical technique which uses the intersection of chords and the second involved an iterative numerical location program. In both location methods, the crust near Socorro was assumed to be a homogeneous half-space with a P-wave velocity of 5.8 km/sec.

Using the above techniques, the actual procedure undertaken to locate the events was the following: A line with a slope of 0.732 was fitted to the plot of S-P times versus P-arrivals for an event. The point at which the line crosses the abscissa was noted because this point was used as an initial origin time estimate. This initial estimate of the origin time was inserted in the iterative location program. Once an iterative solution was obtained, the origin time found from the iterative solution was used to obtain a graphical solution. If the two solutions agreed the location was finalized, if they did not, the origin time was changed to obtain a best fit from the graphical technique. Once a best fit was obtained, the location and origin time were finalized.

Distribution of Microearthquake Epicenters

The epicenters for the 50 located microearthquakes

used in this study are plotted in Figure 3. Corresponding locations and origin times are listed in Table 2.

The major structural features which exhibit microearthquake activity are (1) the area near or within the Socorro Basin centered approximately 5 km north-northwest of Socorro, (2) the southwestern margin of Socorro Mountain, and (3) the southern end of the La Jencia Basin (Figure 3).

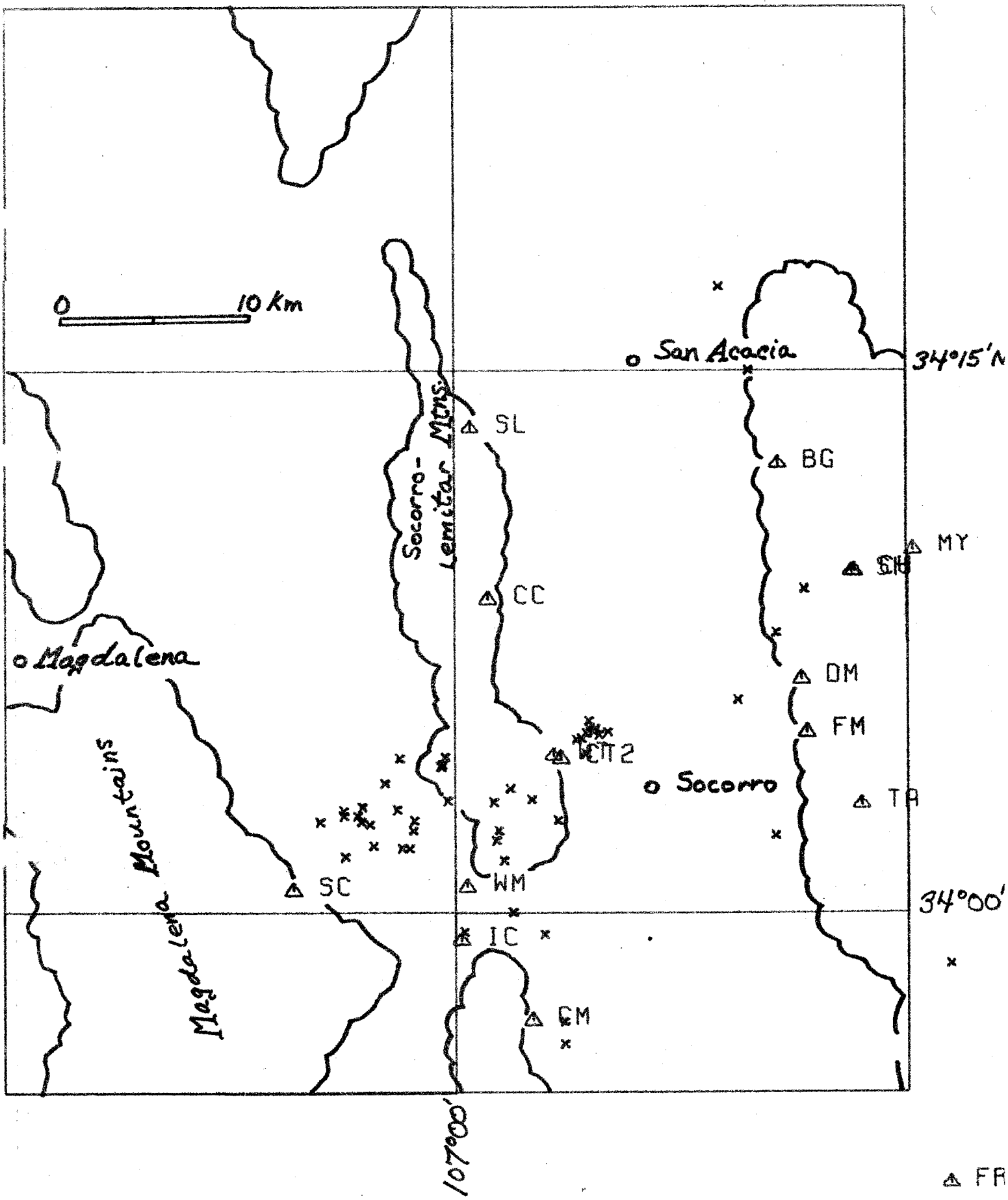

Figure 3. Epicenters of the 50 events used in this study.

Table 2. Microearthquakes Locations, Origin Times, and Poisson's Ratios.

DATE	ITERATIVE ORIGIN TIME	LATITUDE	LONGITUDE	DEPTH	LOCATION GRADE	POISSON'S RATIO
05-22-75	11:36:29.03	33.9397	106.9395	4.70	G	.259
05-22-75	13:19:41.40	33.9500	106.9400	N/A	P	.266
06-03-75	15:10:15.60	34.0301	107.0296	9.50	E	.273
07-30-75	21:44:42.10	34.0848	106.9223	8.20	G	.266
08-05-75	02:26:02.50	34.0335	106.9772	7.60	G	.262
08-05-75	04:17:20.92	34.0379	106.9758	7.80	G	.284
08-08-75	10:53:58.00	34.0837	106.9233	6.70	G	.272
08-08-75	10:57:22.59	34.0796	106.9329	6.80	E	.277
08-12-75	07:09:11.15	34.0357	106.8225	0.0	G	.250
08-12-75	15:25:28.30	34.0513	106.9785	8.80	E	.323
08-13-75	05:19:18.20	34.0823	106.9207	7.30	G	.255
08-13-75	07:39:18.40	34.0826	106.9274	7.90	G	.269
08-13-75	11:22:26.90	34.0245	106.9731	9.10	G	.253
08-20-75	05:16:39.70	34.0882	106.9261	10.10	E	.238
08-20-75	12:20:52.35	34.0833	106.9153	7.00	E	.286
08-20-75	15:29:36.60	34.0848	106.9261	6.90	E	.248
08-21-75	03:44:48.70	34.0407	107.0470	9.50	G	.264
08-21-75	19:04:06.50	34.0575	106.9692	7.50	E	.273
08-29-75	08:52:18.80	34.0737	106.9271	7.20	E	.278
09-16-75	13:30:52.55	34.0804	106.9301	6.70	G	.238
11-04-75	16:30:12.10	34.0491	107.0517	10.00	G	.194
11-05-75	22:28:26.70	34.0424	107.0228	4.50	G	.312
11-07-75	08:27:36.10	34.0480	107.0323	7.10	G	.218
01-27-76	08:37:44.73	34.1290	106.8220	8.90	E	.275
01-27-76	10:05:24.07	34.1490	106.8060	9.60	G	.245
01-29-76	15:06:40.70	34.0000	106.9680	6.50	E	.269
02-17-76	06:17:49.07	34.0450	107.0620	10.20	E	.252
02-17-76	17:34:05.13	34.0520	107.0040	8.20	G	.307
02-18-76	23:25:35.22	34.0420	107.0520	6.20	G	.216
02-19-76	00:08:36.77	34.0260	107.0610	8.60	E	.252
02-20-76	12:51:45.10	34.0310	107.0450	N/A	P	.280
03-18-76	14:45:16.00	33.9760	106.7260	N/A	P	.259
03-18-76	18:34:51.00	34.0420	107.0750	6.10	G	.213
03-23-76	12:53:20.55	34.2500	106.8370	N/A	P	.149
03-25-76	10:50:54.65	34.0425	106.9435	5.50	E	.290
04-13-76	09:45:40.73	34.0720	107.0050	6.10	G	.277
04-13-76	11:41:25.73	34.0450	107.0540	11.40	G	.238
04-13-76	11:58:34.65	33.9900	106.9510	6.40	G	.230
04-13-76	23:15:15.00	34.0300	107.0250	6.00	G	.247
04-14-76	01:50:28.91	33.9910	106.9950	9.10	E	.214
04-14-76	13:12:21.50	34.0710	107.0310	N/A	P	.288
04-15-76	08:45:52.70	34.0680	107.0080	3.60	G	.307
04-15-76	18:28:37.46	34.0521	106.9574	4.80	G	.283
04-16-76	05:34:38.85	34.0380	107.0230	6.10	E	.325
04-16-76	09:33:43.03	34.0670	107.0070	6.60	E	.290
04-16-76	14:07:33.47	34.0686	107.0067	6.90	G	.320
04-20-76	02:52:19.33	34.0470	107.0620	N/A	P	.230

Table 2. continued

DATE	ITERATIVE ORIGIN TIME	LATITUDE	LONGITUDE	DEPTH	LOCATION GRADE	POISSON'S RATI
04-20-76	08:32:19.19	34.0980	106.8430	4.00	E	.221
04-21-76	11:16:20.17	34.2880	106.8530	N/A	P	.294
04-23-76	05:57:59.97	34.0600	107.0390	N/A	P	.278

Data

A complete listing of the data used in this study can be found in Appendix I. Note that only those microearthquakes which were recorded at a minimum of five stations were used in this study.

In the data set, the P-wave arrival times were read with a traveling microscope by Richard P. Mott (1976) and/or Eric J. Rinehart (1976), but double-checked by the author with a millimeter scale. All of the S-P intervals were measured carefully with a traveling microscope by the author. Each S-P interval was graded according to its readability and the grading system was as follows:

E= excellent- very sharp P and S phases with no noise obscuring the beginning of the phases.

G= good- a little noise obscuring the phases, but the beginnings of the P and S phases obvious.

F= fair- some noise in data, amplitudes are such that the S pick is somewhat subjective, but not unreasonable.

P= poor- S phase somewhat obscure, but picked by a change in frequency and/or change in amplitude.

A one standard deviation reading error associated with the P-arrival time is estimated by Rinehart (1976) to be about .03 sec. The one standard deviation reading error associated with the S-P intervals are grade-dependent; the poorer the grade, the larger the respective

reading error. The following one standard deviation reading errors for the S-P intervals were estimated by the author: (1) E (.02 sec.), (2) G (.04 sec), (3) F (.06 sec.), and (4) P (.09 sec.).

Some of the events in the data set were not assigned a depth as can be seen from Table 2. In this study, the locations of each of the 50 events were assigned a grade of either excellent (E), good (G), or poor (P). The grade, which was assigned by Rinehart (1976), was dependent upon (1) the magnitude of residuals in the iterative location program, (2) the location of the epicenter within or outside of the array, (3) epicentral distance of the nearest seismic station, and (4) the ability to use a reflection off a prominent discontinuity to resolve depth. The above criteria was not met by the grade P locations and therefore no reliable depths could be assigned.

Eighty-four percent of the events used in this study were graded either good or excellent. The other 16 percent were kept in the data set for several reasons: (1) the data set was already limited by the requirement of 5 or 6 station locations and (2) the S-P intervals and P-arrivals were not necessarily poor on these events and thus they could be used in the analysis of the average Poisson's ratio for the Socorro region.

Finally, it must be noted that the data set used in this study was fixed as of October, 1976. Continuing studies at New Mexico Institute of Mining and Technology

could subject this data set to change. Before the data used in this study is put to any future use one should check to see if any subsequent changes have been made.

Previous Studies of Poisson's Ratio Near Socorro

A study of the ratio of P-wave velocity to S-wave velocity and Poisson's ratio was conducted in the Rio Grande Rift, between Albuquerque and Socorro, N.M., by Kiet Sakdejayont (1974). Thirty-two well-recorded micro-earthquakes within 45 km of the Socorro station were used in his study. The Poisson's ratio and Vp/Vs ratio were found to be 0.217 and 1.664, respectively. These two comparatively low values were considered by Sakdejayont to be normal values for the Rio Grande Rift.

Poisson's Ratio From Seismic Observations

Procedure

Figure 4 is a plot of S-P times versus P-arrival times for several events recorded by this survey. These plots are called Wadati diagrams. Note that the plot of S-P intervals versus P-arrival gives a straight line with a slope of $(\alpha/\beta - 1)$ which come from the relation

where $(S-P) = (P-O)(\alpha/\beta - 1)$,
S= S-wave arrival time,
P= P-wave arrival time,
O= Origin time of the microearthquake,
α= P-wave velocity,
β= S-wave velocity.

A Wadati diagram was drawn and a linear regression analysis performed to find Poisson's ratio associated with each event. This was done by using the slope of the straight line to find the velocity ratio α/β. The equation connecting the velocity ratio (α/β) and Poisson's ratio is

$$\gamma = \frac{(\alpha^2/\beta^2 - 2)}{2(\alpha^2/\beta^2 - 1)}.$$

Figure 5 is a graph of this relationship between Poisson's ratio and the velocity ratio. Marked on this graph is the often assumed value of Poisson's ratio of 0.25.

Results

Poisson's ratio was computed for all of the 50 events used in this study. The results are listed in Table 2. The mean value of Poisson's ratio was found to be 0.262

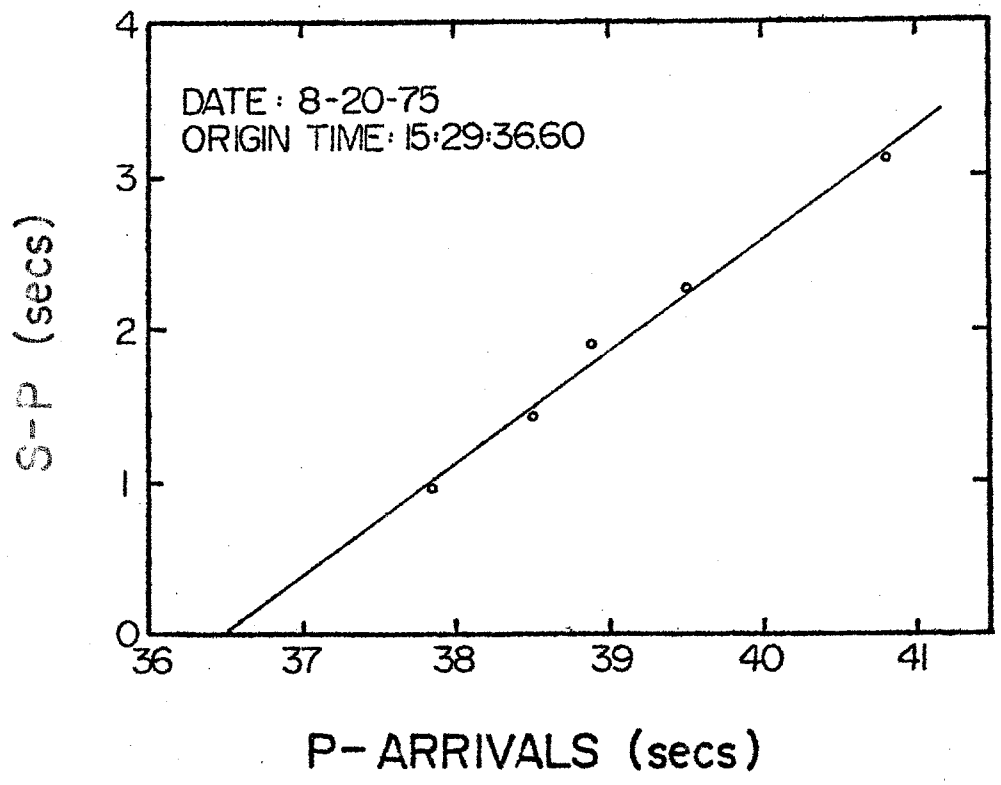

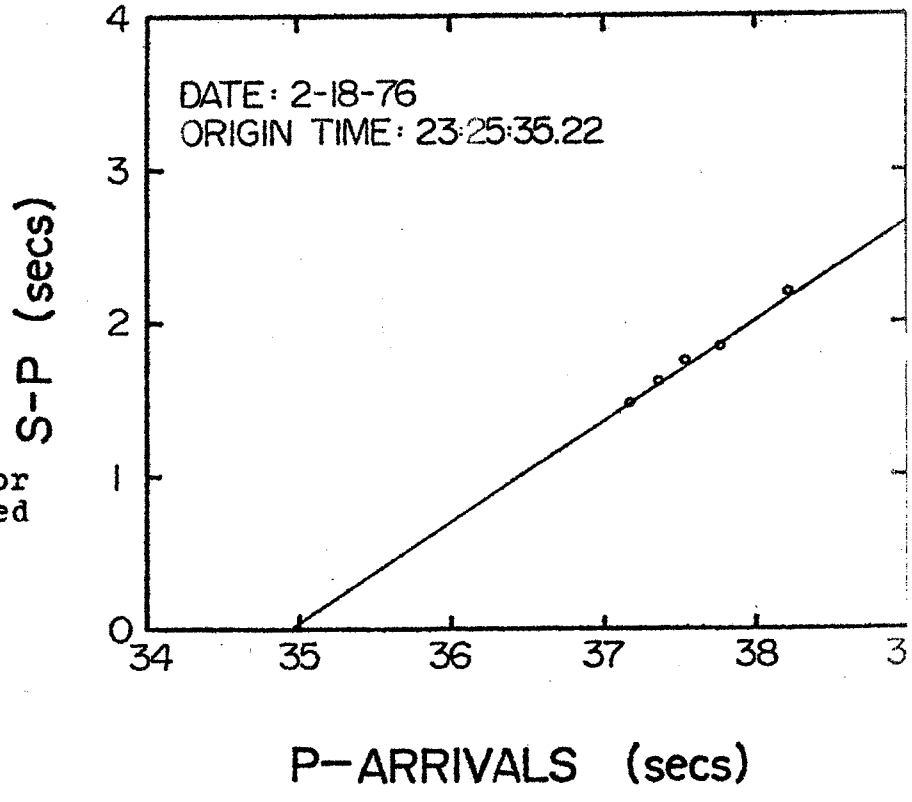

Figure 4. Wadati diagrams for two events recorded in this survey.

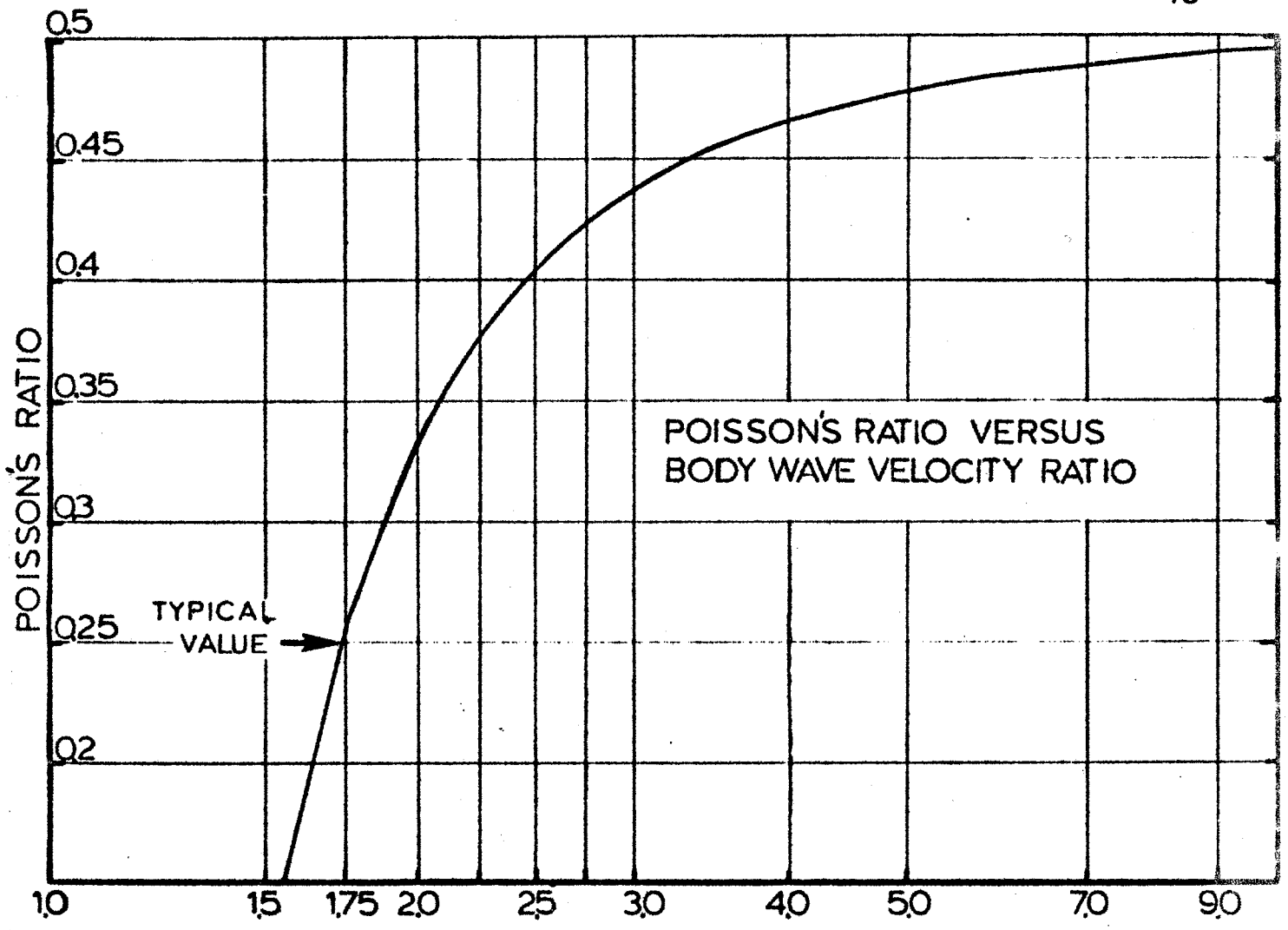

Figure 5. The relationship between Poisson's ratio and the velocity ratio (α/β).

with a standard deviation of 0.034. The epicenters for the 50 microearthquakes and their associated Poisson's ratios are plotted in Figure 6. The figure shows a dispersed Poisson's ratio picture with no apparent pattern. One might suggest that Poisson's ratio is decreasing away from the major activity areas, but this observation is purely subjective.

Two origin times were found for each event. One was found by the method discussed in the Location of Microearthquake Procedure section, which hereafter will be called the iterative origin time because most of them were generated by the iterative location program. The second was found using a linear regression analysis of the straight line plots of P-arrivals versus S-P intervals or Wadati diagrams for each event (Table 3). The iterative origin time for each event was compared with the Wadati origin time. Most of the iterative origin times fell within the 95 percent confidence intervals of the Wadati origin times. The events for which the iterative origin time and Wadati origin time did not agree had one or two special characteristics; either the S-P picks were very poor, which resulted in the dropping of that event from the data set or one or more stations exhibited an early arrival time or large S-P interval which probably pushed the 95 percent confidence interval out of its normal range. For an example of the second case, see Figure 7. Events of the type shown in Figure 7 were kept in the data set because their P-arrivals

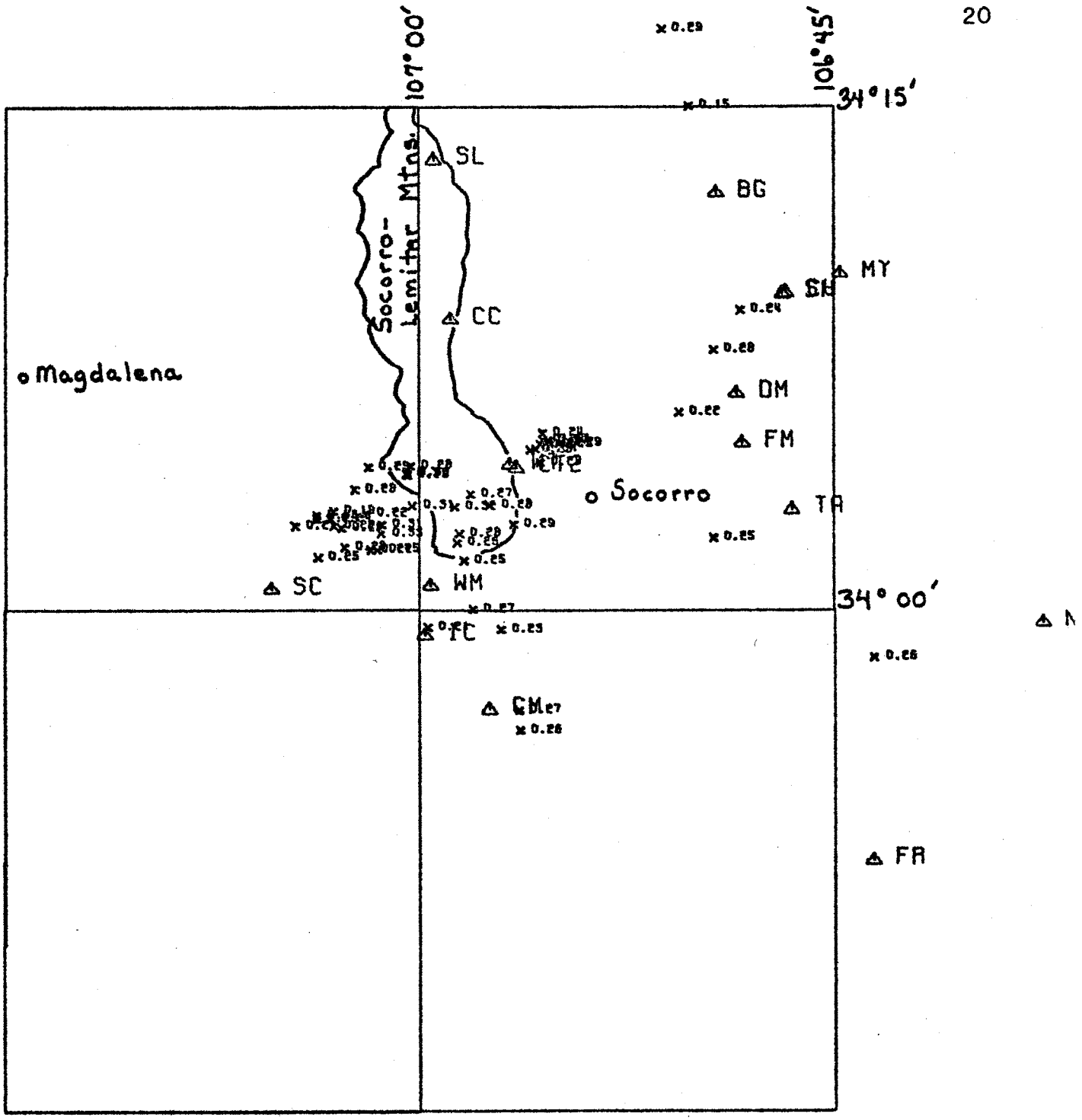

Figure 6. A plot of the 50 epicenters and their associated Poisson's ratios.

Table 3. A list of the Wadati origin times and relevant statistical information for the 50 events in this study.

DATE	WADATI ORIGIN TIME	SLOPE	STANDARD DEVIATION OF THE SLOPE	CORRELATION COEFFICIENT	POISSON'S RATIO
05-22-76	11:36:28.86	0.7538	0.0506	0.9933	0.259
05-22-76	13:19:41.35	0.7703	0.0216	0.9988	0.266
06-03-75	15:10:15.61	0.7894	0.0630	0.9906	0.273
07-30-75	21:44:42.08	0.7701	0.0385	0.9963	0.266
08-05-75	02:26:02.29	0.7621	0.0366	0.9966	0.262
08-05-75	04:17:21.00	0.8214	0.0736	0.9882	0.284
08-08-75	10:53:57.93	0.7880	0.0269	0.9983	0.272
08-08-75	10:57:22.36	0.7999	0.0428	0.9957	0.277
08-12-75	07:09:10.57	0.7318	0.0625	0.9857	0.250
08-12-75	15:25:28.95	0.9565	0.1053	0.9822	0.323
08-13-75	05:19:18.18	0.7432	0.0356	0.9954	0.255
08-13-75	07:39:18.51	0.7781	0.0382	0.9952	0.269
08-13-75	11:22:26.69	0.7402	0.0397	0.9957	0.253
08-20-75	05:16:39.69	0.7061	0.0316	0.9970	0.238
08-20-75	12:20:52.56	0.8255	0.0520	0.9941	0.286
08-20-75	15:29:36.47	0.7271	0.0439	0.9946	0.248
08-21-75	03:44:48.79	0.7671	0.0658	0.9892	0.264
08-21-75	19:04:06.38	0.7891	0.0723	0.9877	0.273
08-29-75	08:52:18.79	0.8032	0.0592	0.9919	0.278
09-16-75	13:30:52.26	0.7049	0.0165	0.9992	0.238
11-04-75	16:30:11.16	0.6236	0.0169	0.9989	0.194
11-05-75	22:28:26.65	0.9144	0.0223	0.9991	0.312
11-07-75	08:27:35.55	0.6652	0.0607	0.9877	0.218
01-27-76	08:37:44.75	0.7961	0.0526	0.9935	0.275
01-27-76	10:05:24.01	0.7207	0.0163	0.9992	0.245
01-29-76	15:06:40.38	0.7793	0.0587	0.9889	0.269
02-17-76	06:17:49.05	0.7364	0.0768	0.9843	0.252
02-17-76	17:34:05.66	0.8942	0.1464	0.9621	0.307
02-18-76	23:25:34.95	0.6623	0.0317	0.9954	0.216
02-19-76	00:08:36.78	0.7363	0.0926	0.9691	0.252
02-20-76	12:51:45.43	0.8091	0.1246	0.9642	0.280
03-18-76	14:45:16.37	0.7531	0.0432	0.9935	0.259
03-18-76	18:34:50.53	0.6567	0.0415	0.9940	0.213
03-23-76	12:53:17.80	0.5576	0.0760	0.9732	0.149
03-25-76	10:50:54.32	0.8387	0.0178	0.9993	0.290
04-13-76	09:45:40.71	0.8005	0.0543	0.9907	0.277
04-13-76	11:41:25.30	0.7053	0.1008	0.9613	0.238
04-13-76	11:58:34.52	0.6893	0.0232	0.9977	0.230
04-13-76	23:15:14.93	0.7256	0.0447	0.9944	0.247
04-14-76	01:50:28.44	0.6585	0.2088	0.8443	0.214
04-14-76	13:12:21.28	0.8332	0.0835	0.9852	0.288
04-15-76	08:45:52.93	0.8943	0.0327	0.9974	0.307
04-15-76	18:28:37.36	0.8179	0.0396	0.9964	0.283
04-16-76	05:34:39.22	0.9653	0.0540	0.9953	0.325
04-16-76	09:33:43.13	0.8394	0.0641	0.9884	0.290
04-16-76	14:07:33.82	0.9451	0.1004	0.9779	0.320
04-20-76	02:52:19.09	0.6890	0.0094	0.9997	0.230

Table 3. continued

DATE	WADATI ORIGIN TIME	SLOPE	STANDARD DEVIATION OF THE SLOPE	CORRELATION COEFFICIENT	POISSON'S RATIO
04-20-76	08:32:18.76	0.6712	0.0712	0.9835	0.221
04-21-76	11:16:19.81	0.8508	0.1332	0.9543	0.294
04-23-76	05:57:59.56	0.8027	0.0598	0.9918	0.278

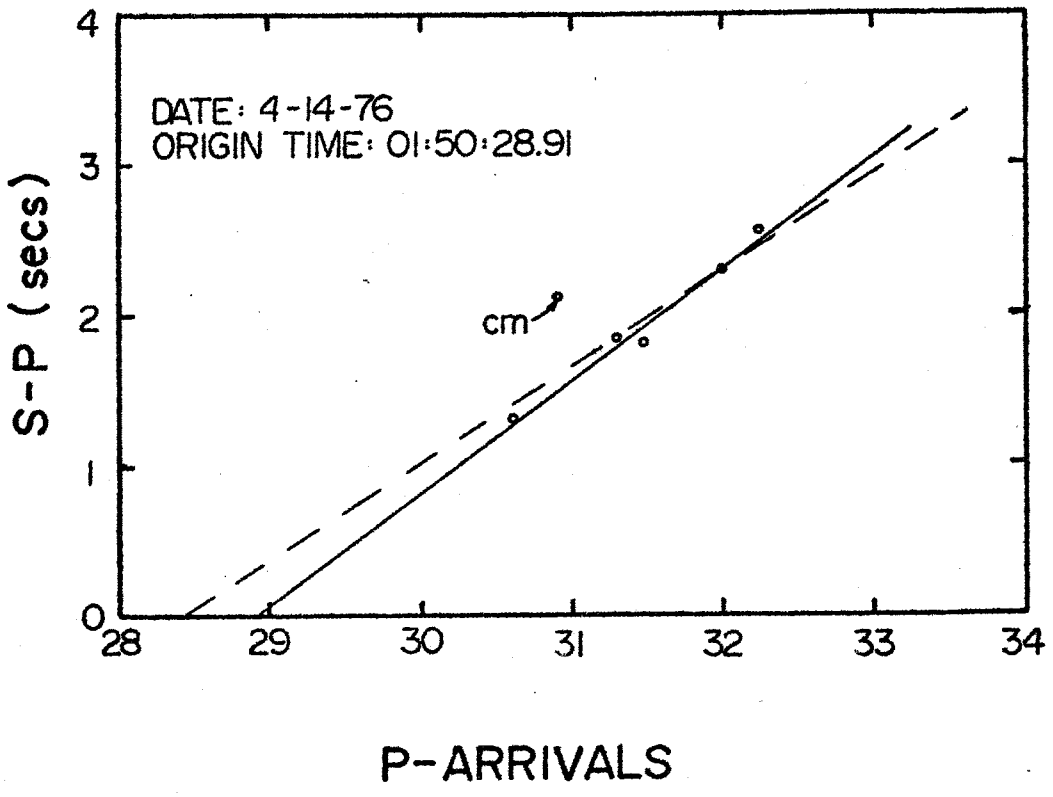

Figure 7. An example of an event which exhibited an early arrival time or large S-P interval. The dashed line is the best fit line including station CM. The solid line is the best fit line excluding station CM.

and S-P intervals were thought to be just as good or better than the P-arrivals and S-P intervals associated with other events used in this study.

In discussing the two origin times, some observations need to be made. First, the iterative origin time is based on a minimum residual concept using a half-space crustal model with a P-wave velocity of 5.8 km/sec. Second, Wadati origin times have somewhat large confidence intervals due to the small number of data points and the fact that the S-P intervals are of variable quality. At this point one might ask which origin time is best suited for use in the Socorro area? Considering the large variations in Poisson's ratio, as can be seen from Table 2, one might think that the Wadati origin time is best because the velocity variations in the array are averaged. In discussing this point, just the opposite argument can be put forth. The large variations in Poisson's ratio in the Socorro region must indicate large variations in the S-wave velocity, because a number of observations suggest that a P-wave velocity of 5.8 km/sec is close to the true velocity (Toppozada and Sanford, 1976). Taking into account the small variation in the P-wave velocity, and large variations in the S-wave velocity, the iterative origin time, which minimizes the residuals assuming a P-wave velocity of 5.8 km/sec, is without question the best estimate of the microearthquake origin time.

Finally, an attempt was made to correlate Poisson's ratio with hypocenter depth. Figure 8 is a plot of

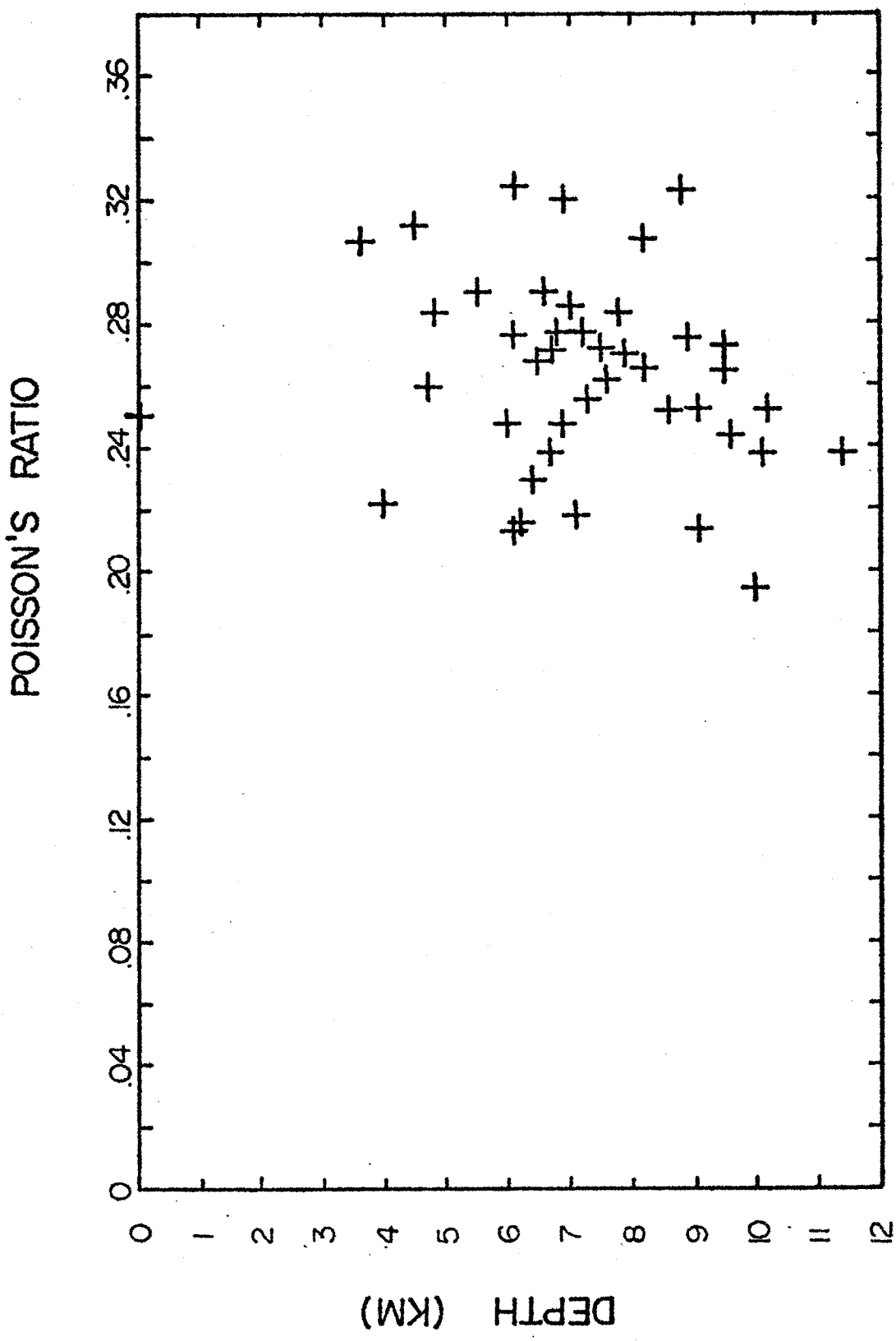

Figure 8. The plot of depth of focus versus Poisson's ratio for the 42 events graded good or excellent.

Poisson's ratio versus hypocenter depth for the 42 events graded good or excellent. A linear regression analysis was applied to the data in this figure and a correlation coefficient of 0.17 was obtained. This correlation coefficient indicates that no linear correlation between Poisson's ratio and hypocenter depth exists.

Statistical Variation of Poisson's Ratio

In order to determine the statistical variation in Poisson's ratio, correlation coefficients and 95 percent confidence intervals on the slope were included in the linear regression analysis. Of the 50 events, the best computed correlation coefficient was 0.9997 and the 95 percent confidence interval on Poisson's ratio was $\pm$ 0.012. Despite the almost perfect straight line fit, the small number of data points created a statistical scatter in the slope. In this type of study on Poisson's ratio, a large number of stations will give a greater statistical confidence in the results, except in the case where the distribution of the stations with respect to the hypocenters results in the S-P intervals being very similar. The equations used in the above analysis are listed and discussed briefly in Appendix II.

Spatial Distribution of Poisson's Ratio

Procedure

Before discussing the technique used to find the spatial distribution of Poisson's ratio in the Socorro area, the basic equation in this study should be reviewed:

$$(S-P) = (P-O)(\alpha/\beta - 1)$$

In addition to giving an estimate of the origin time of the event this equation also yields information about the velocity ratio without requiring the development of travel-time curves or the location of the seismic sources. However, each individual raypath from a microearthquake focus to the receiving stations can be assigned a characteristic velocity ratio and/or Poisson's ratio depending on the average physical parameters of the earth between the points. Because of this, the velocity ratio and Poisson's ratio obtained for a specific microearthquake is an average for the different travel paths in the array (Figure 9). To determine the velocity ratio and/or Poisson's ratio for an area more directly, a new method, herein called the raypath technique, was devised.

To find the spatial distribution of Poisson's ratio from the raypath technique, composite Wadati diagrams were constructed. The actual construction procedure was as follows: (1) an imaginary circle around each of the

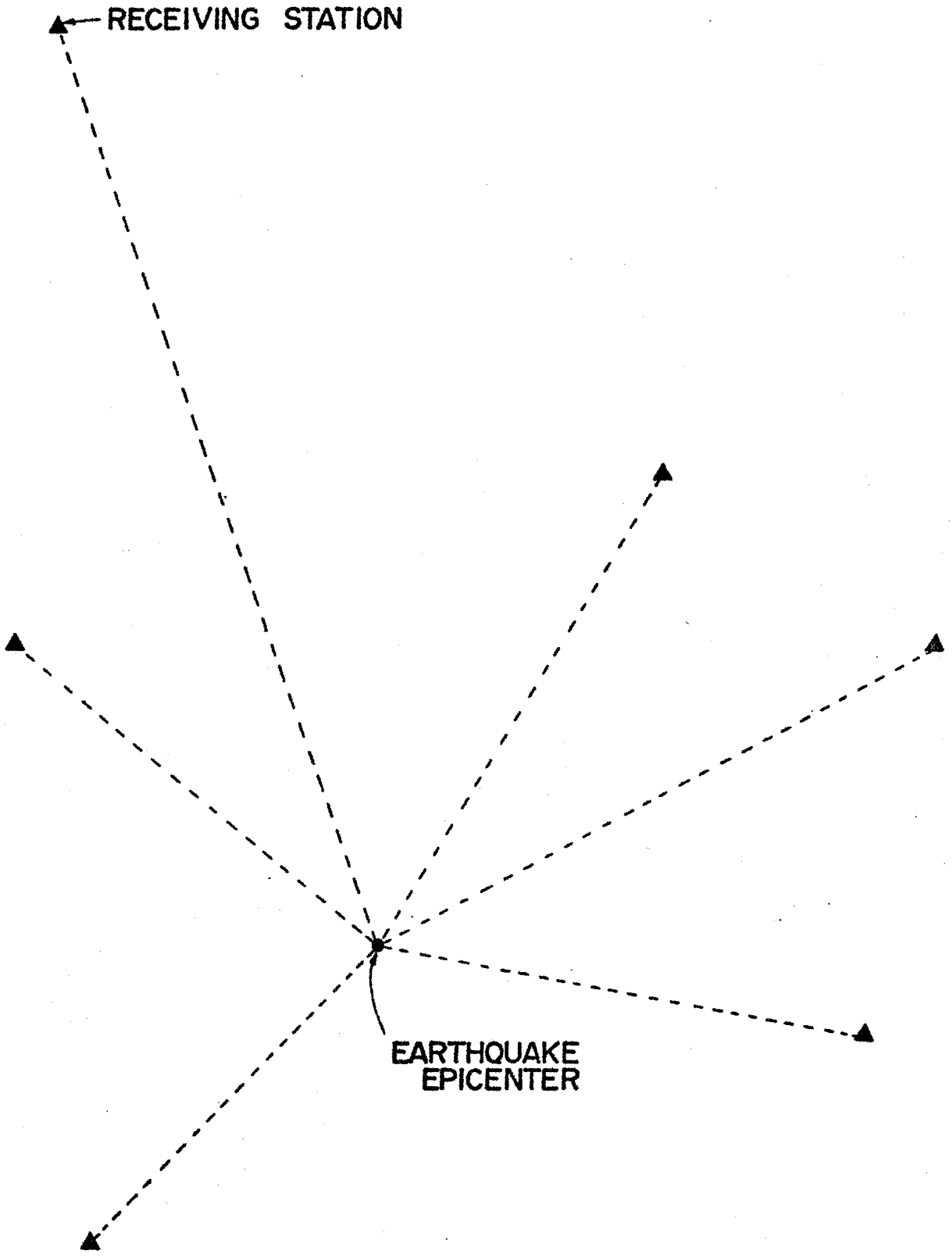

Figure 9. A typical array used in a microearthquake survey.

receiving stations was drawn, (2) the circle was divided into 10 degree increments (the number of degrees in an increment would be dependent on the area of study, amount of microearthquake activity, and the personal preference of the researcher), (3) the S-P intervals of raypaths which lie within each wedge-shaped crustal segment around the station were plotted against their P-wave travel times, and (4) a linear regression analysis, assuming the line must pass through the 0.0 point, was performed on the data points to find the velocity ratio and thus Poisson's ratio for each crustal segment at each receiving station. A minimum of three data points were required for each crustal segment, i.e. at least two travel paths, before a linear regression analysis was performed. It is important to note again that each increment used the point 0.0 as one of its data points because 0.0 corresponds to the origin time of all events in the analysis. Thus the lines of best fit had to rotate about the 0.0 point (Figure 10).

This iterative process is quite adaptable to the computer and two parameters, latitude and longitude, or three parameters, latitude, longitude, and depth of focus, may be used to construct a Poisson's ratio model for an area. Because of the limited data set, the author chose to ignore depth of focus and found two parameter Poisson's ratio models for the Socorro area.

Socorro Raypath Analysis

Two types of raypath computations were undertaken for

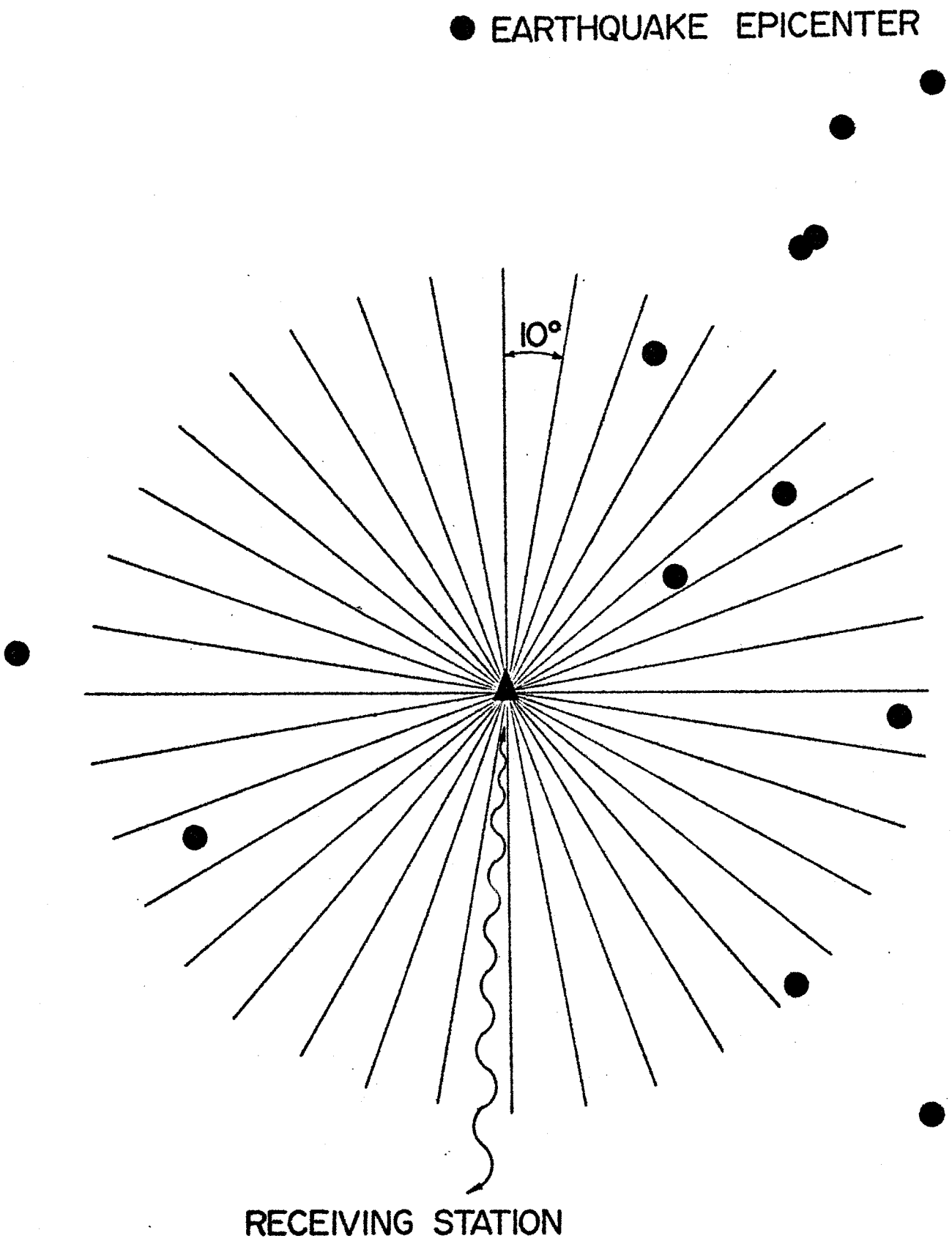

Figure 10. The distribution of crustal wedges used in the study of the spatial distribution of Poisson's ratio for a seismic receiving station.

the Socorro area, one based on the iterative origin times and the other based on origin times obtained from Wadati diagrams. The Wadati origin times were generated by fitting a line with a slope of 0.756 (γ= 0.26) to a Wadati diagram for each event.

Figure 11 shows the results of the Socorro raypath analysis using iterative origin times and 10 degree increments of the crust around each station. Note only 9 stations of the total 17 were occupied long enough to accumulate enough data for this type of analysis.

Since the raypath technique is new, the actual interpretation of the results is quite subjective. It was decided to first look at areas defined by intersecting crustal increments from two or more stations, each increment having a Poisson's ratio significantly higher ($\geq$0.28) than the average found for the Socorro area. Three such anomalous areas were defined. They are: (1) southern La Jencia Basin with an average Poisson's ratio of 0.292, (2) Socorro Mountain with an average Poisson's ratio of 0.289, and (3) central La Jencia Basin with an average Poisson's ratio of 0.284 (Figure 12). Again these areas were defined by intersections of crustal sections which exhibit high Poisson's ratios and the locations of the microearthquakes were ignored. To allow a more detailed interpretation, the hypocenters lying within each of the crustal wedges defining the anomalies are plotted in Figures 13, 14, and 15.

In Figure 13, the crustal wedges defining the southern

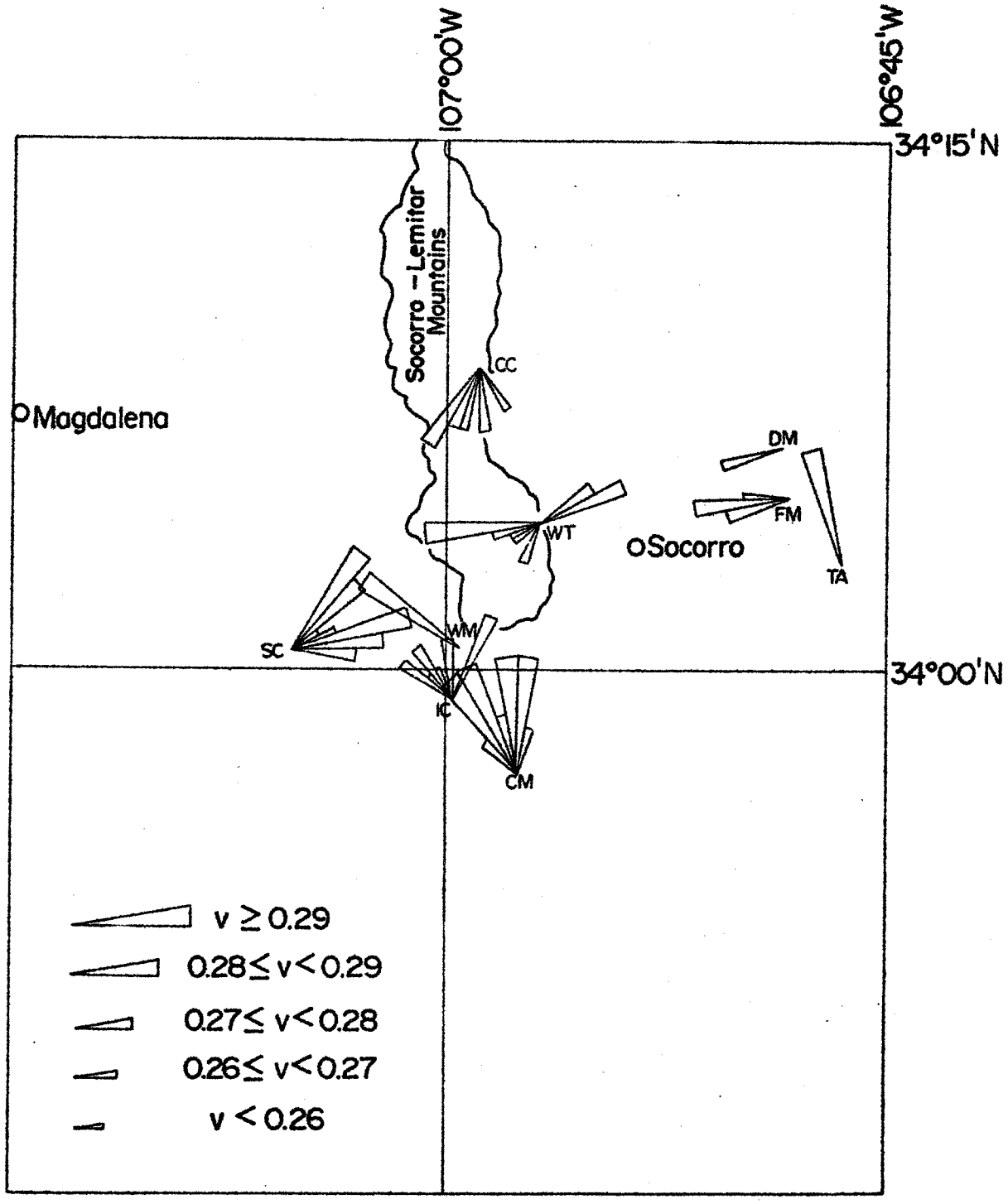

Figure 11. The spatial distribution of Poisson's ratio in the Socorro region from iterative origin time data.

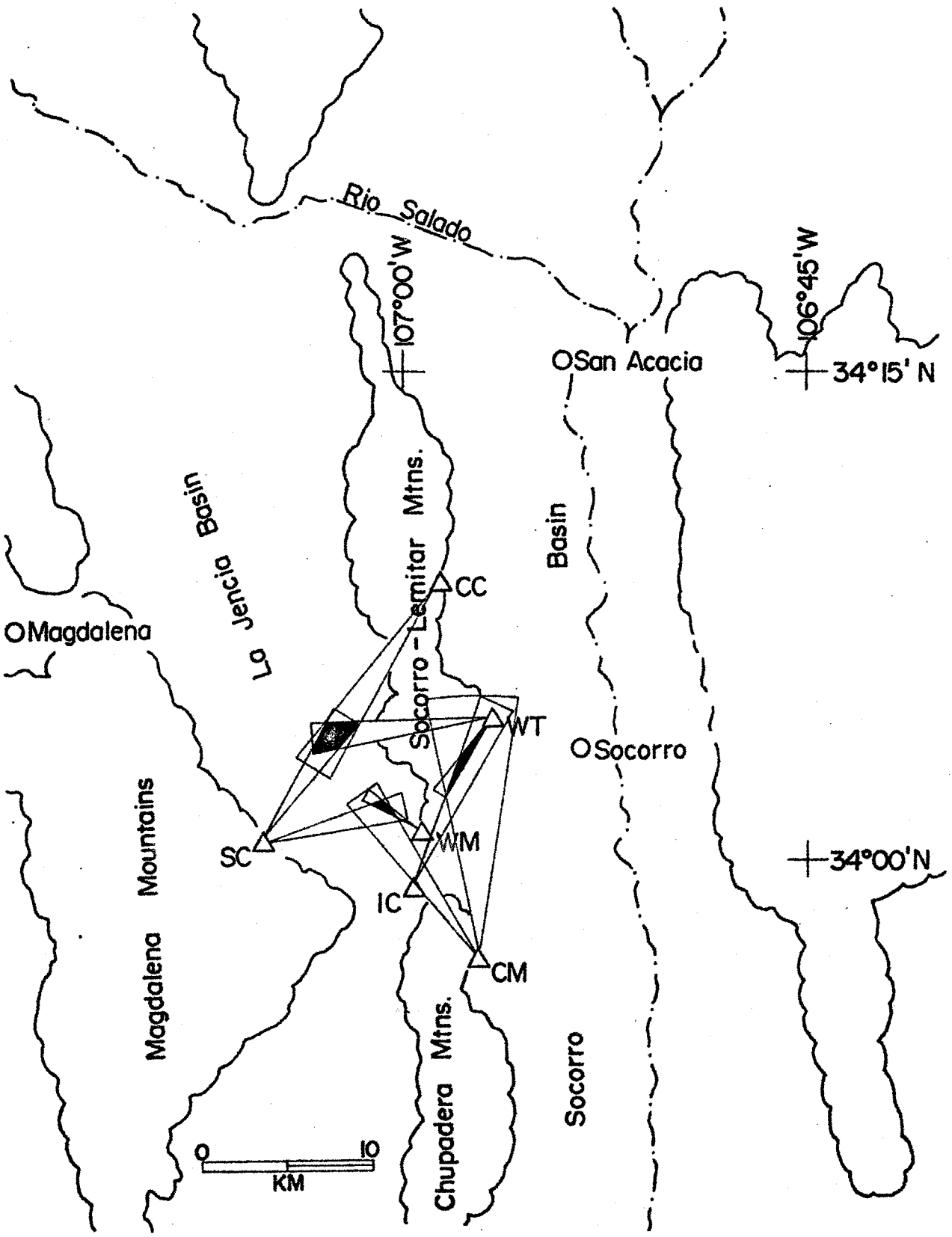

Figure 12. Three anomalous areas in the Socorro region defined by intersecting crustal wedges.

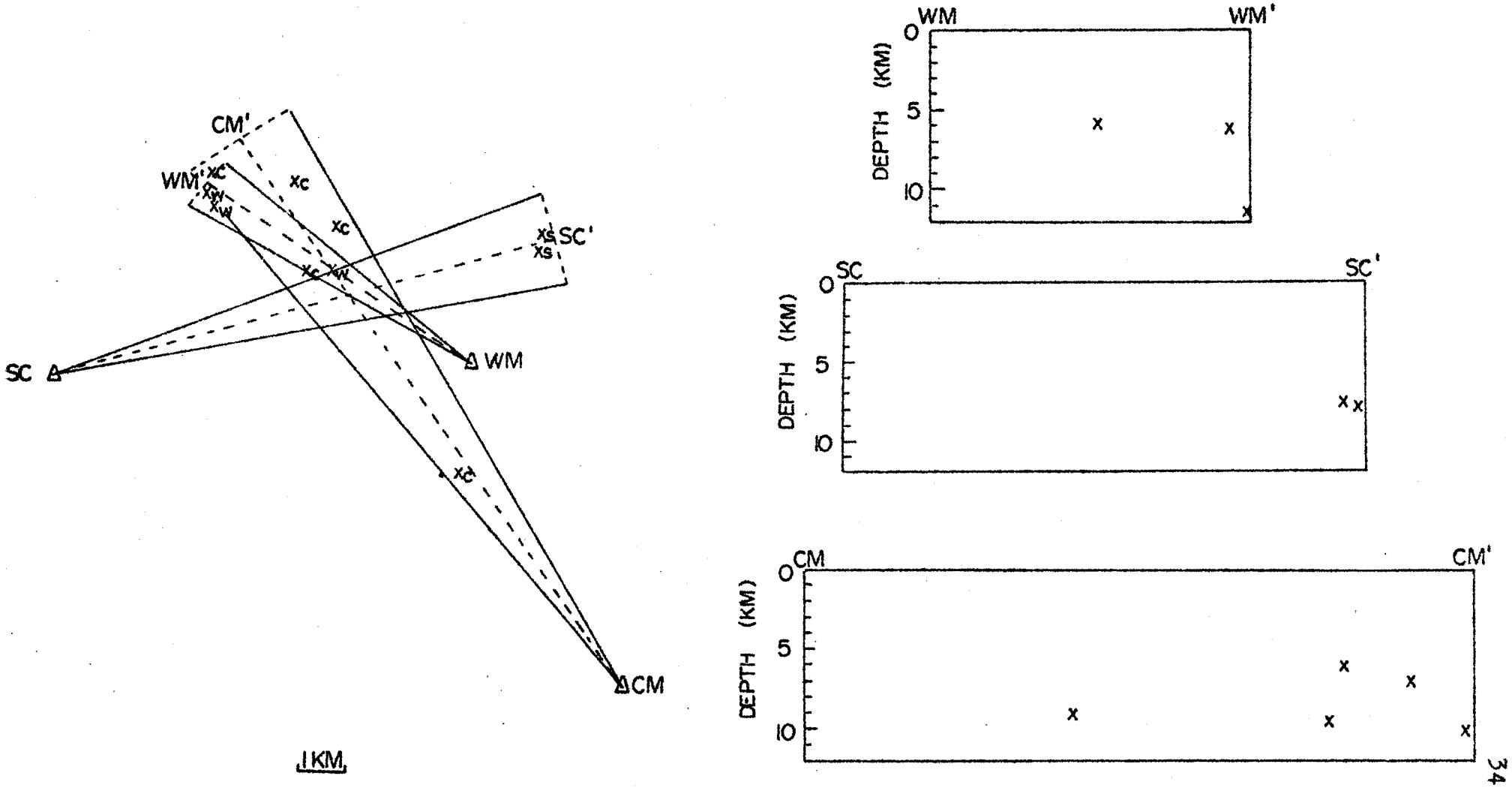

Figure 13. Locations of the hypocenters in the crustal wedges used to define the southern La Jencia Basin anomaly.

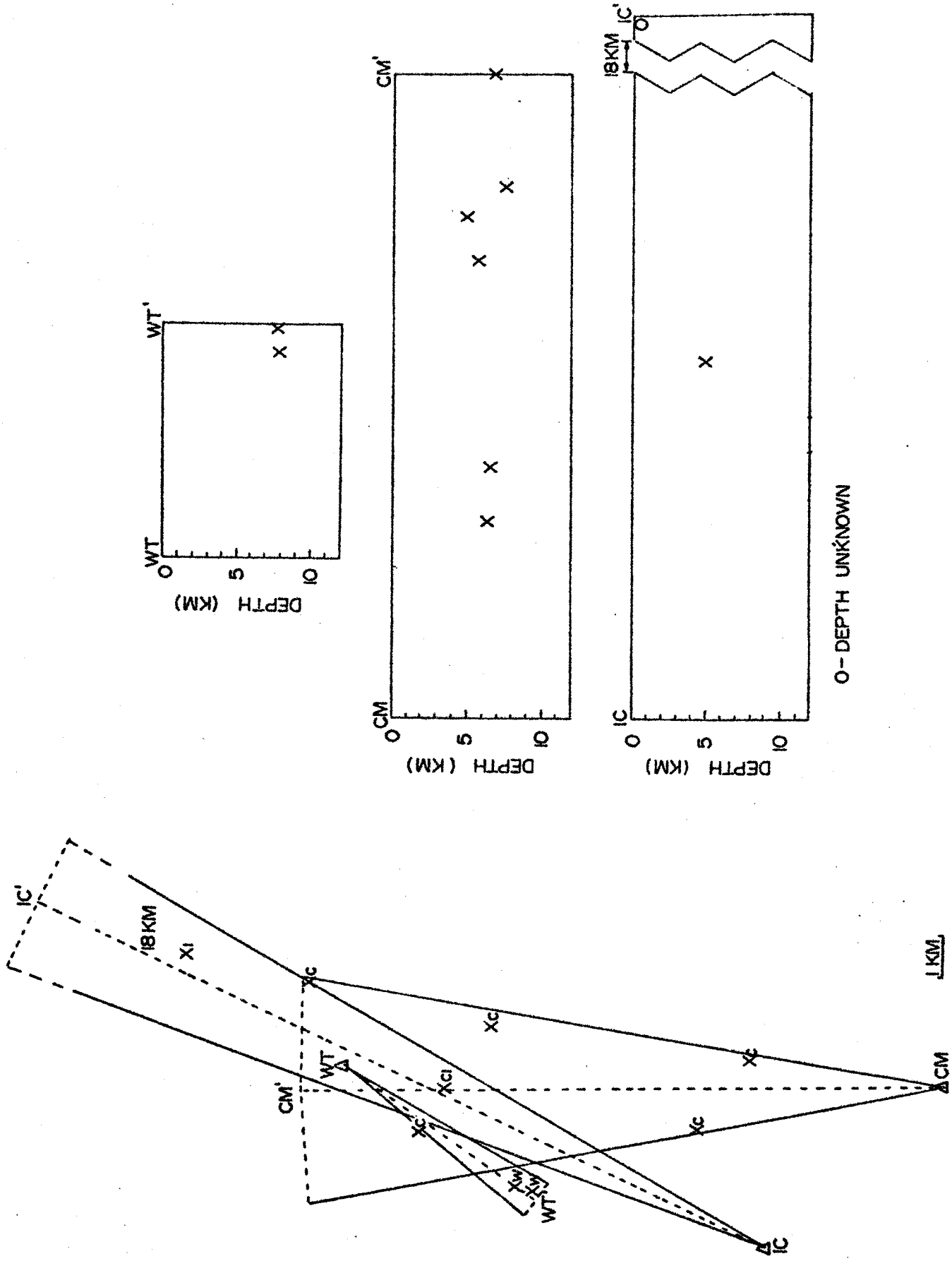

Figure 14. Locations of the hypocenters in the crustal wedges used to define the Socorro Mountain anomaly.

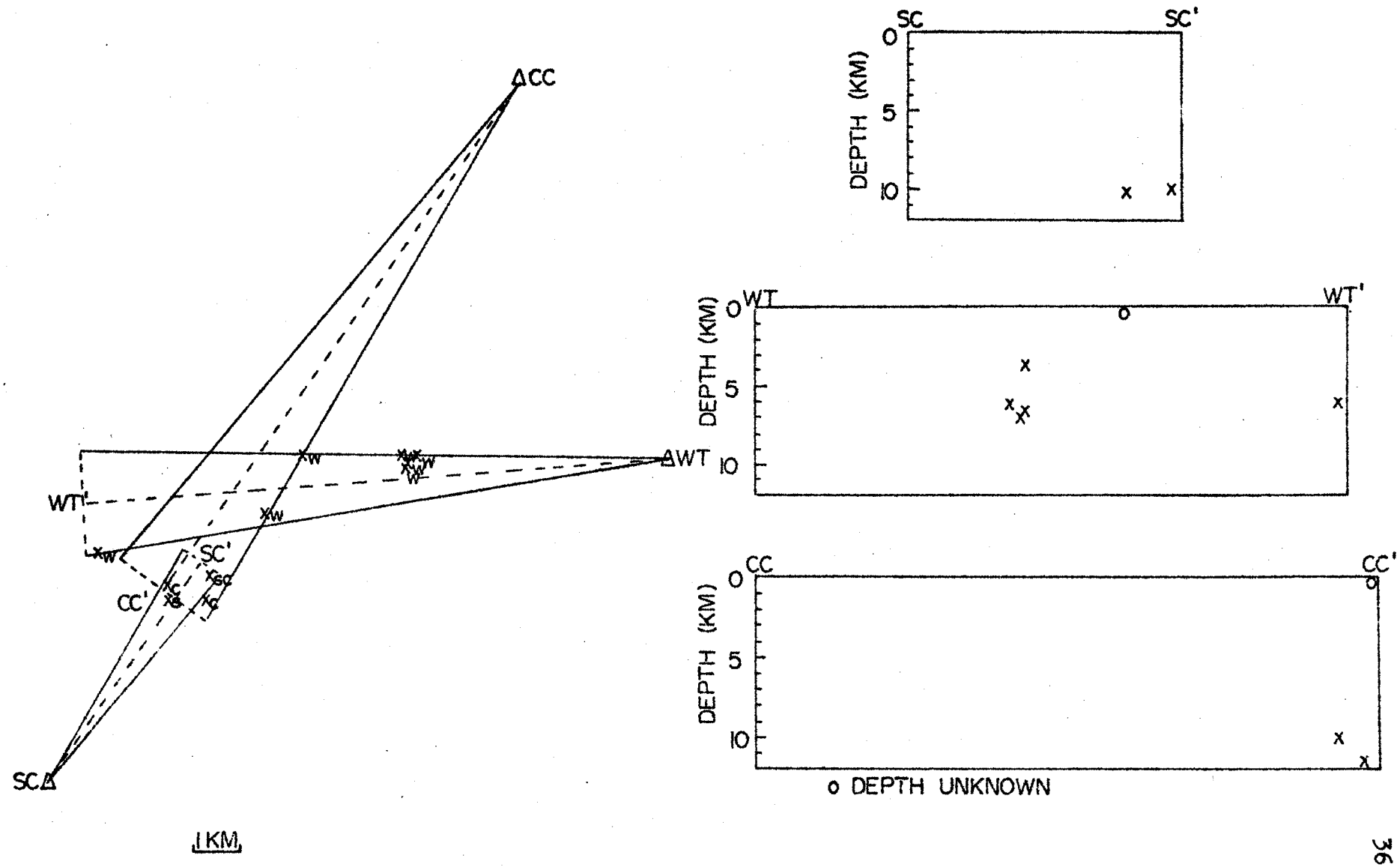

Figure 15. Locations of the hypocenters in the crustal wedges used to define the central La Jencia Basin anomaly.

La Jencia Basin anomaly indicate that all but one of the raypaths from the earthquake foci traverse the proposed anomalous area. This observation strengthens the case for an anomalous body in the southern La Jencia Basin.

Figure 14 shows the intersecting crustal wedges which define an anomalous region beneath Socorro Mountain. Examination of the hypocenter locations in this figure indicates that an anomalous body is not defined by the intersections of the crustal segments. The hypocenters in the two increments northward from station CM which exhibit Poisson's ratios of 0.306 and 0.311 respectively, are all, except for one, south of the intersection area. A more likely location for an anomalous body would be an area south of Socorro Mountain and north of station CM. With the number of events in the two increments it is hard to say at this time exactly where the anomalous area exists, but Shuleski's (1976) S-wave screening anomaly near station CM would be consistent with the Poisson's ratio observations.

The last anomaly defined by intersecting crustal sections can be seen in Figure 15. Note that most of the microearthquakes in the defining increments are on the station side of the anomaly and the raypaths would not traverse it. This observation indicates little chance that an anomaly exists in central La Jencia Basin. One could propose several anomalous areas to explain the high observed Poisson's ratios, but the author believes this would be too speculative with the data set at hand.

At this point the data is inadequate to isolate other anomalous regions, but Figures 16 through 18 are plots of those crustal sections (with hypocenters) in the Socorro area which exhibited significantly high Poisson's ratios ($\geq$0.28). These individual increments could be used to compliment observations in any future study.

The second type of raypath computation undertaken for the Socorro area, as mentioned earlier, was based on the Wadati origin times. This phase of the study was undertaken because it was thought that the Wadati diagrams might give a better estimate of a microearthquake origin time than the iterative origin time. The iterative numerical location program was used to relocate the 50 events after constraining the origin times to the calculated Wadati origin times. The new locations and origin times are listed in Table 4. New travel times and azimuths were also calculated for the 50 events for use in the Socorro raypath analysis.

As can be seen from Figure 19, a Poisson's ratio of 0.26 used to calculate the Wadati origin times is reflected in the raypath analysis results using these origin times. The largest value of Poisson's ratio in any increment is 0.291 at WT (20-30). Other increments having significantly high values are: (1) WT (60-70) with a Poisson's ratio of 0.280 and (2) CM (320-330) with a Poisson's ratio of 0.288. From this analysis, only the southern La Jencia Basin anomaly can be supported.

To possibly indicate any general geographic trends

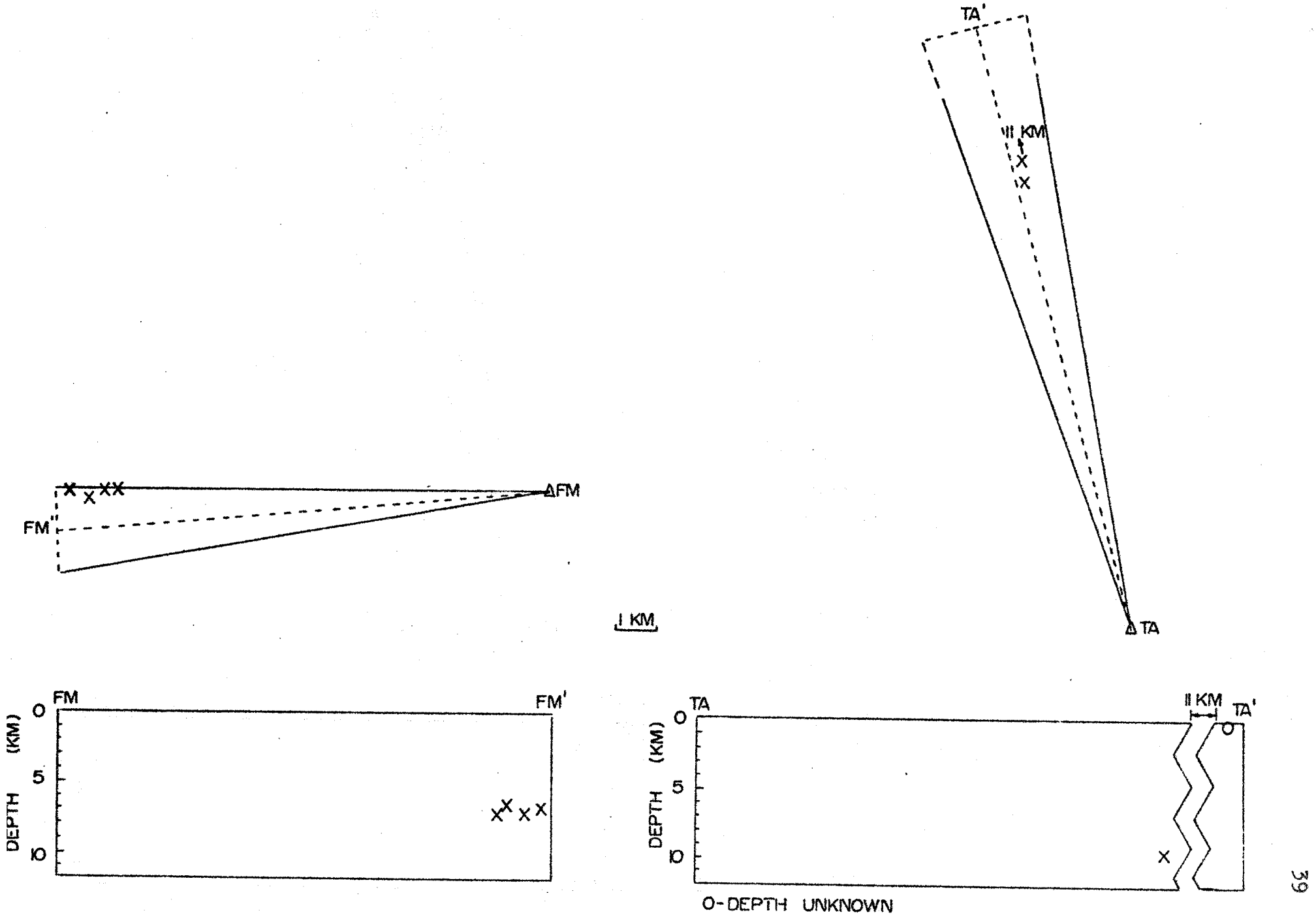

Figure 16. Locations of the hypocenters in the crustal wedges which exhibited significantly high Poisson's ratios (Station Fm, 260-270), (Station TA, 340-350).

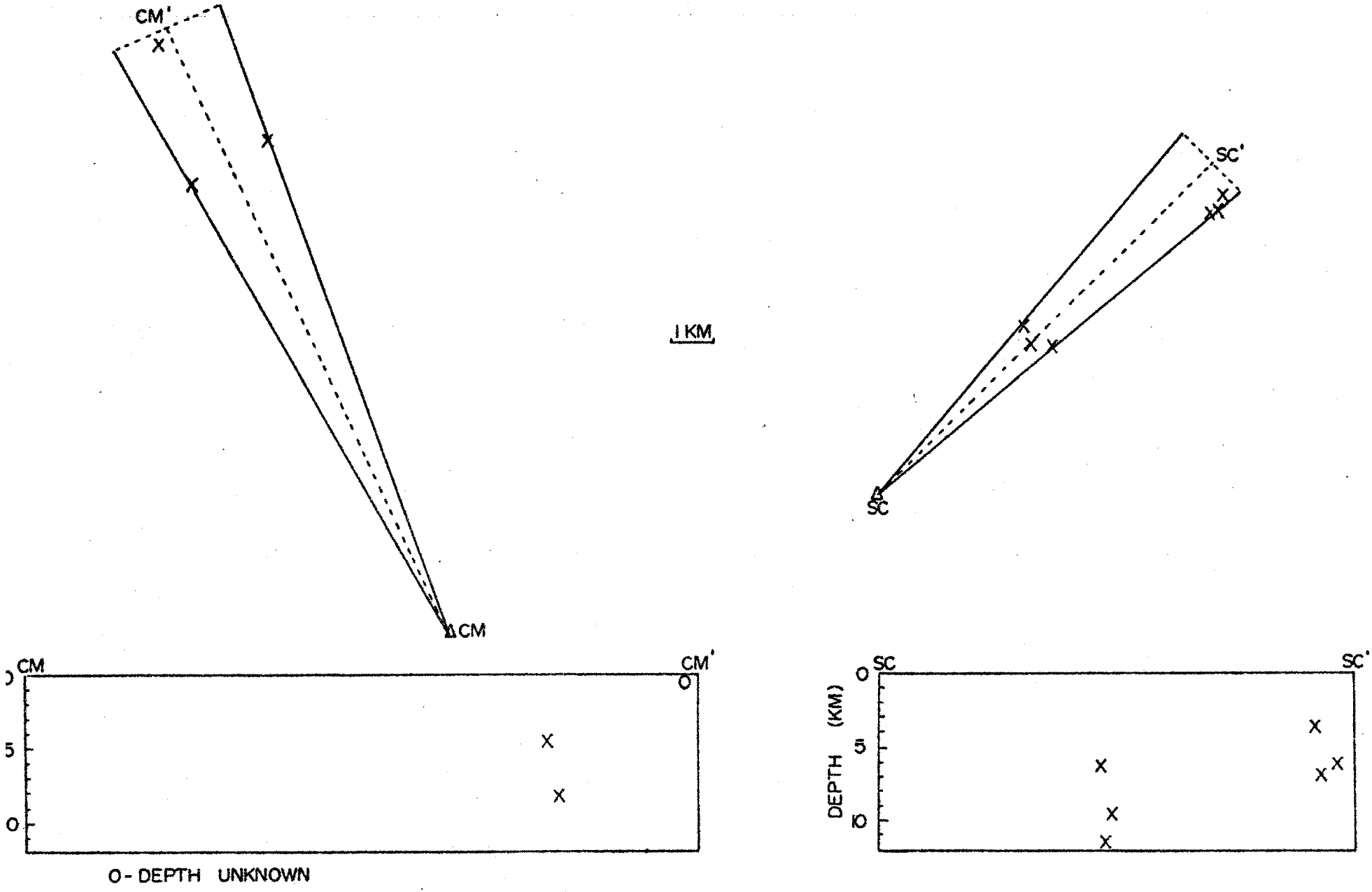

Figure 17. Locations of the hypocenters in the crustal wedges which exhibited significantly high Poisson's ratios (Station CM, 330-340), (Station SC, 40-50).

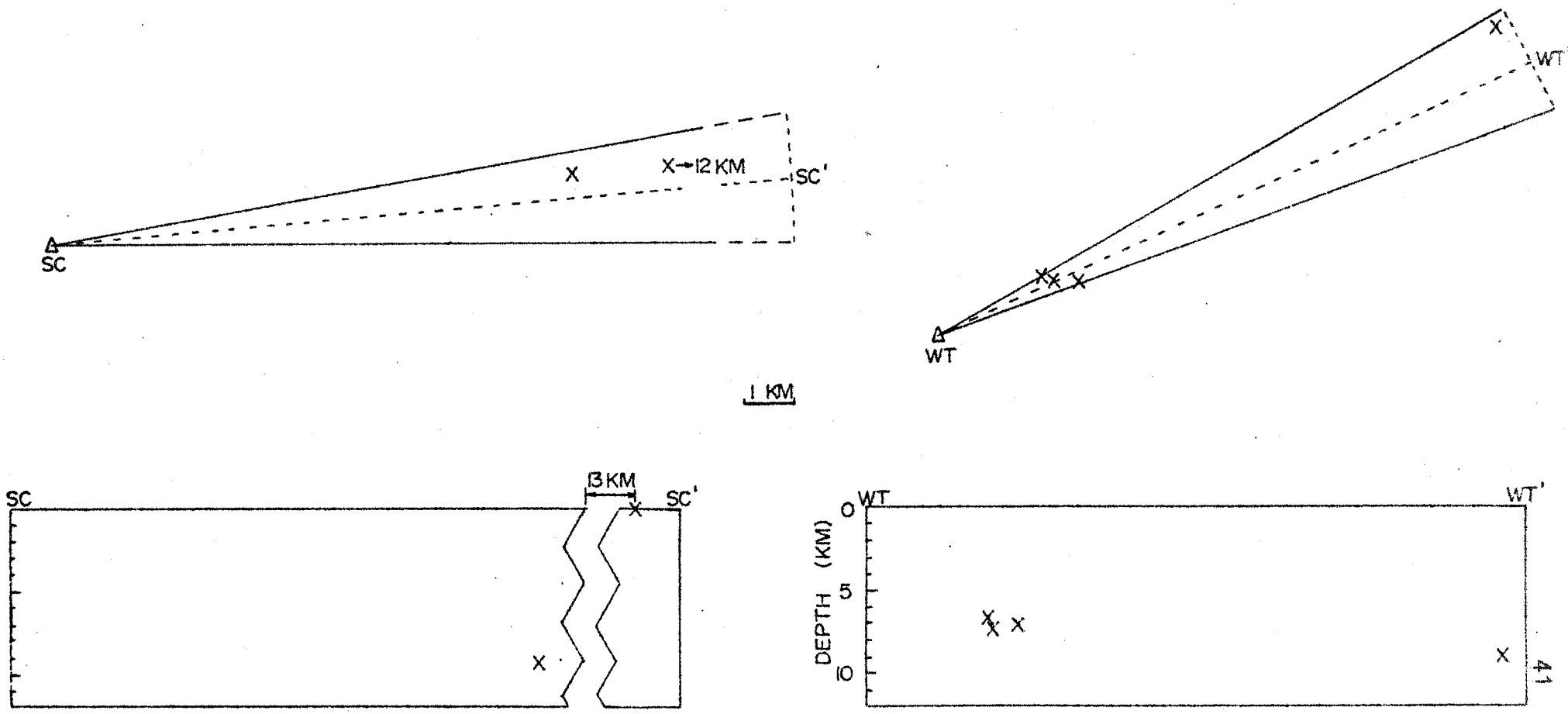

Figure 18. Locations of the hypocenters in the crustal wedges which exhibited significantly high Poisson's ratios (Station SC, 80-90), (Station WT, 60-70).

Table 4. Locations Obtained by Constraining the Origin Times to the Forced Wadati Origin Times.

DATE	FORCED WADATI ORIGIN TIME	LATITUDE	LONGITUDE	DEPTH
05-22-75	11:36:28.86	33.9356	106.9392	3.18
05-22-76	13:19:41.29	33.9392	106.9337	4.11
06-03-75	15:10:15.49	34.0294	107.0338	8.54
07-30-75	21:44:42.04	34.0860	106.9255	7.65
08-05-75	02:26:02.27	34.0336	106.9783	8.20
08-05-75	04:17:20.81	34.0371	106.9840	7.17
08-08-75	10:53:57.83	34.0843	106.9211	6.34
08-08-75	10:57:22.23	34.0856	106.9325	6.84
08-12-75	07:09:10.67	34.0347	106.7982	4.33
08-12-75	15:25:28.48	34.0504	106.9784	5.96
08-13-75	05:19:18.23	34.0816	106.9244	7.02
08-13-75	07:39:18.43	34.0839	106.9269	6.72
08-13-75	11:22:26.75	34.0228	106.9753	8.28
08-20-75	05:16:39.89	34.0821	106.9075	9.66
08-20-75	15:29:36.57	34.0856	106.9268	5.99
08-20-75	12:20:52.38	34.0815	106.9132	4.18
08-21-75	03:44:48.75	34.0413	107.0463	6.97
08-21-75	19:04:06.27	34.0575	106.9742	8.04
08-29-75	08:52:18.64	34.0771	106.9262	6.98
09-16-75	13:30:52.54	34.0818	106.9281	5.44
11-04-75	16:30:11.81	34.0490	107.0643	6.55
11-05-75	22:28:26.11	34.0439	107.0577	6.80
11-07-75	08:27:36.07	34.0452	107.0266	4.99
01-27-76	08:37:44.59	34.1238	106.8039	9.33
01-27-76	10:05:24.16	34.1492	106.8076	7.64
01-29-76	15:06:40.30	33.9914	106.9732	5.94
02-17-76	06:17:49.12	34.0442	107.0604	8.04
02-17-76	17:34:05.33	34.0516	107.0023	7.74
02-18-76	23:25:35.29	34.0401	107.0623	8.13
02-19-76	00:08:36.84	34.0272	107.0577	8.04
02-20-76	12:51:45.28	34.0287	107.0375	8.54
03-18-76	14:45:16.38	33.9813	106.7269	5.98
03-18-76	18:34:51.02	34.0403	107.0658	6.34
03-23-76	12:53:19.85	34.2946	106.8231	7.55
03-25-76	10:50:54.01	34.0561	106.9693	8.72
04-13-76	09:45:40.59	34.0729	107.0038	5.49
04-13-76	11:41:25.47	34.0440	107.0601	7.88
04-13-76	11:58:34.71	33.9908	106.9522	4.67
04-13-76	23:15:15.00	34.0327	107.0253	3.31
04-14-76	01:50:28.80	33.9887	106.9953	9.32
04-14-76	13:12:21.09	34.0705	107.0296	5.33
04-15-76	08:45:52.61	34.0695	107.0065	6.01
04-15-76	18:28:37.20	34.0566	106.9526	6.51
04-16-76	05:34:38.86	34.0400	107.0200	4.30
04-16-76	09:33:42.94	34.0670	107.0064	5.20
04-16-76	14:07:33.43	34.0688	107.0065	4.96
04-20-76	02:52:19.45	34.0407	107.0707	4.59
04-20-76	08:32:19.05	34.0948	106.8369	3.54
04-21-76	11:16:19.40	34.2928	106.8398	8.77
04-23-76	05:57:59.34	34.0384	107.0672	6.83

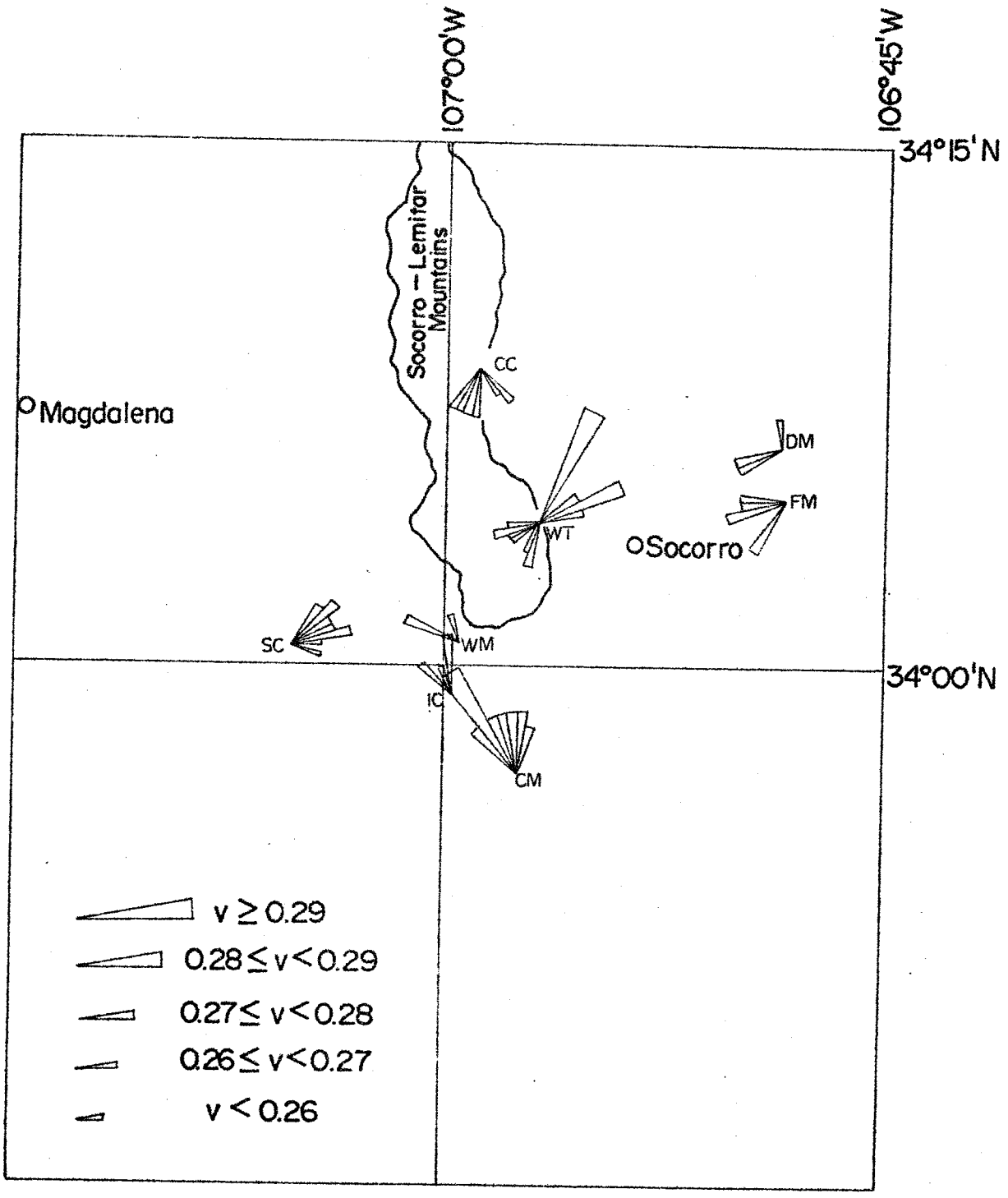

Figure 19. The spatial distribution of Poisson's ratio in the Socorro region from data with Wadati origin times.

of Poisson's ratio in the Socorro region, an average Poisson's ratio was found for each station. The method used to calculate each station's average involved taking a crustal segment's Poisson's ratio and multiplying that number by the number of data points in that increment so that a weighted average would be taken. The results using iterative origin time data are:

CM= 0.283
CC= 0.268
FM= 0.269
TA= 0.304 1 increment
IC= 0.263
WM= 0.258
DM= 0.267
SC= 0.270
WT= 0.267

Overall the averages are quite high. Stations CM and SC, which are near the two proposed anomalous areas, have the highest Poisson's ratios.

The average Poisson's ratio for each station using Wadati origin time data are:

TA= 0.244 1 increment
DM= 0.258
FM= 0.263
IC= 0.257
WM= 0.259
CC= 0.257
CM= 0.268
WT= 0.257
SC= 0.259

Using the Wadati origin times, the average Poisson's ratio for each station is very near the original 0.26 used to calculate the origin times.

Variations of Poisson's Ratio in the Raypath Technique

One should be aware that the results of the Socorro raypath analysis just discussed are subject to statistical

uncertainty. As can be seen in Appendix III, which lists the raypath results and associated 95 percent confidence intervals, the small number of data points in the crustal segments produces relatively large 95 percent confidence intervals on the slopes of the composite Wadati diagrams and thus on the Poisson's ratios. Other possible weaknesses in the Socorro raypath results could be reading errors and possibly errors in microearthquake origin times. However, the author believes that if one has confidence in the methods used to determine the origin times of the events in this study, the Socorro raypath results gives values of Poisson's ratio which are representative of the region.

Discussion of the Factors Which Affect Poisson's Ratio

Four main factors influence Poisson's ratio: (1) fractures (fluid or gas-filled), (2) pressure, (3) temperature, and (4) composition. These factors will be described and related to the observed Poisson's ratio anomalies found in this study.

Fractures

Nur and Simmons (1969) measured velocities in dry as well as saturated samples of fractured rock. They assumed that the effective elastic constants are related to the velocities in the same way that these quantities are related in a linear elastic material. Thus the effective dynamic bulk modulus is

$$K = \rho(Vp^2 - 4/3Vs^2),$$

and the effective dynamic shear modulus is

$$\mu = \rho Vs^2.$$

Poisson's ratio obtained for both the dry and saturated cases is

$$\gamma = ((Vp/Vs)^2/2((Vp/Vs)^2-1),$$

where Vp= P-wave velocity,
Vs= S-wave velocity,
ρ = Density of sample.

The values in Table 5 emphasize the observation that fluid saturation greatly influences the effective bulk modulus of the fractured rock while the shear modulus remains essentially unchanged (Figure 20). Also from

Table 5. Effective Elastic Constants for Dry and Water Saturated Rocks (Nur and Simmons, 1969).

Pressure (bars)	μ (dry) mb	μ (sat.) mb	K (dry) mb	K (sat.) mb	E (dry) mb	E (sat.) mb	ν (dry)	ν (sat.)
			Casco granite					
0	0.139	0.132	0.050	0.570	0.250	0.400	-0.100	0.374
50	0.201	0.176	0.250	0.635	0.430	0.550	0.230	0.350
100	0.236	0.204	0.397	0.637	0.523	0.531	0.240	0.335
200	0.262	0.259	0.492	0.641	0.654	0.692	0.278	0.320
400	0.291	0.311	0.560	0.643	0.790	0.760	0.265	0.304
700	0.318	0.340	0.589	0.665	0.856	0.823	0.258	0.294
1000	0.340	0.352	0.627	0.649	0.889	0.869	0.264	0.277
2000	0.358	0.365	0.639	0.647	0.921	0.906	0.260	0.266
3000	0.365	0.371	0.642	0.650	0.934	0.923	0.258	0.263
			Westerly granite					
0	0.208	0.239	0.106	0.478	0.377	0.614	-0.094	0.286
50	0.243	0.251	0.225	0.502	0.515	0.638	0.130	0.285
100	0.250	0.255	0.324	0.522	0.596	0.657	0.194	0.290
200	0.266	0.263	0.392	0.532	0.651	0.577	0.223	0.288
400	0.285	0.276	0.436	0.554	0.702	0.711	0.232	0.286
700	0.297	0.290	0.474	0.570	0.758	0.745	0.240	0.282
1000	0.306	0.297	0.500	0.577	0.761	0.761	0.246	0.280
2000	0.321	0.314	0.545	0.578	0.805	0.797	0.254	0.276
3000	0.328	0.319	0.558	0.583	0.824	0.810	0.254	0.269
			Triy granite					
0	0.236	0.234	0.180	0.520	0.520	0.617	0.065	0.310
50	0.276	0.276	0.475	0.652	0.694	0.726	0.257	0.315
100	0.293	0.293	0.532	0.633	0.741	0.760	0.268	0.300
200	0.309	0.309	0.592	0.647	0.791	0.801	0.277	0.294
400	0.326	0.326	0.626	0.640	0.832	0.835	0.278	0.283
700	0.335	0.335	0.644	0.652	0.856	0.858	0.279	0.281
1000	0.338	0.338	0.647	0.667	0.865	0.869	0.277	0.283
			Webatuck dolomite					
0	0.384	0.378	0.280	0.740	0.950	0.850	0.030	0.275
50	0.404	0.399	0.461	0.740	1.011	0.937	0.161	0.265
100	0.423	0.421	0.611	0.739	1.061	1.032	0.219	0.260
200	0.452	0.443	0.681	0.739	1.109	1.109	0.229	0.250
400	0.472	0.475	0.725	0.729	1.171	1.164	0.232	0.232
700	0.481	0.495	0.732	0.730	1.211	1.184	0.230	0.223
1000	0.489	0.508	0.738	0.731	1.220	1.160	0.229	0.226
2000	0.497	0.520	0.743	0.731	1.261	1.219	0.226	0.215
3000	0.505	0.528	0.745	0.739	1.279	1.235	0.244	0.211
			Bedford limestone					
0	0.605	0.062	0.105	0.470	0.161	0.184	0.247	0.435
50	0.072	0.072	0.120	0.468	0.182	0.207	0.249	0.427
100	0.080	0.081	0.135	0.466	0.201	0.230	0.251	0.418
200	0.096	0.099	0.166	0.462	0.242	0.276	0.257	0.400
400	0.120	0.120	0.213	0.449	0.303	0.330	0.263	0.377
700	0.140	0.136	0.254	0.436	0.355	0.370	0.265	0.360
1000	0.159	0.151	0.290	0.428	0.404	0.405	0.268	0.342
2000	0.188	0.178	0.360	0.407	0.481	0.467	0.277	0.309
			Solenhofen limestone					
0	–	–	–	–	–	–	–	–
50	0.240	0.238	0.516	0.526	0.624	0.621	0.298	0.303
100	0.242	0.241	0.517	0.526	0.627	0.627	0.298	0.301
500	0.250	0.251	0.517	0.533	0.645	0.651	0.291	0.296
1500	0.256	0.256	0.630	0.548	0.662	0.665	0.292	0.298
3000	0.260	0.260	0.535	0.552	0.672	0.673	0.290	0.297

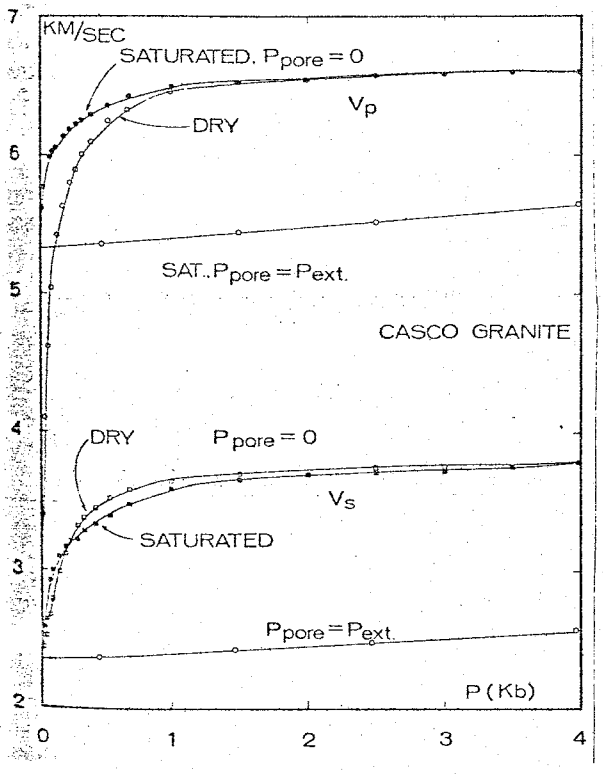

Figure 20. Velocity of elastic waves in Casco granite as a function of pressure. The compressional wave velocity depends significantly on the degree of saturation but shear wave velocity is almost independent (Nur and Simmons, 1969).

Table 5, note that dry fractured rocks exhibit very small, even negative values of Poisson's ratio, while saturated rocks exhibit much higher values.

The Poisson's ratios obtained at various pressures in Table 5 are interesting, but the effect of temperature and pressure on Poisson's ratio will be discussed later in this section.

The Socorro area is a highly fractured region due to its location in the Rio Grande Rift. The interaction of these fractures with ground water might play an important part in the spatial changes in Poisson's ratio in the Socorro area. Hall (1963) located and studied many springs in the Socorro area (Figure 21). Two warm (90-91°F) springs, Sedillo and Socorro, are of particular interest because they have flows in excess of 200gpm, lie on definite fault zones, and discharge water which has traveled through the proposed anomalous area in the southern La Jencia Basin. From the evidence of Nur and Simmons (1969), one could propose this Poisson's ratio anomaly to be caused by water-filled fractures. However, the author does not believe the anomaly to be water-related for the following reasons: (1) the Poisson's ratio anomaly in the southern La Jencia Basin is confined to a relatively small area ($\sim$ 2-3 km^2), rather than extending along the path of the water from recharge areas to the discharge area at the springs, (2) ground water occurs in all of the Socorro region, as can be seen in Figure 21, yet, Poisson's ratio anomalies are quite

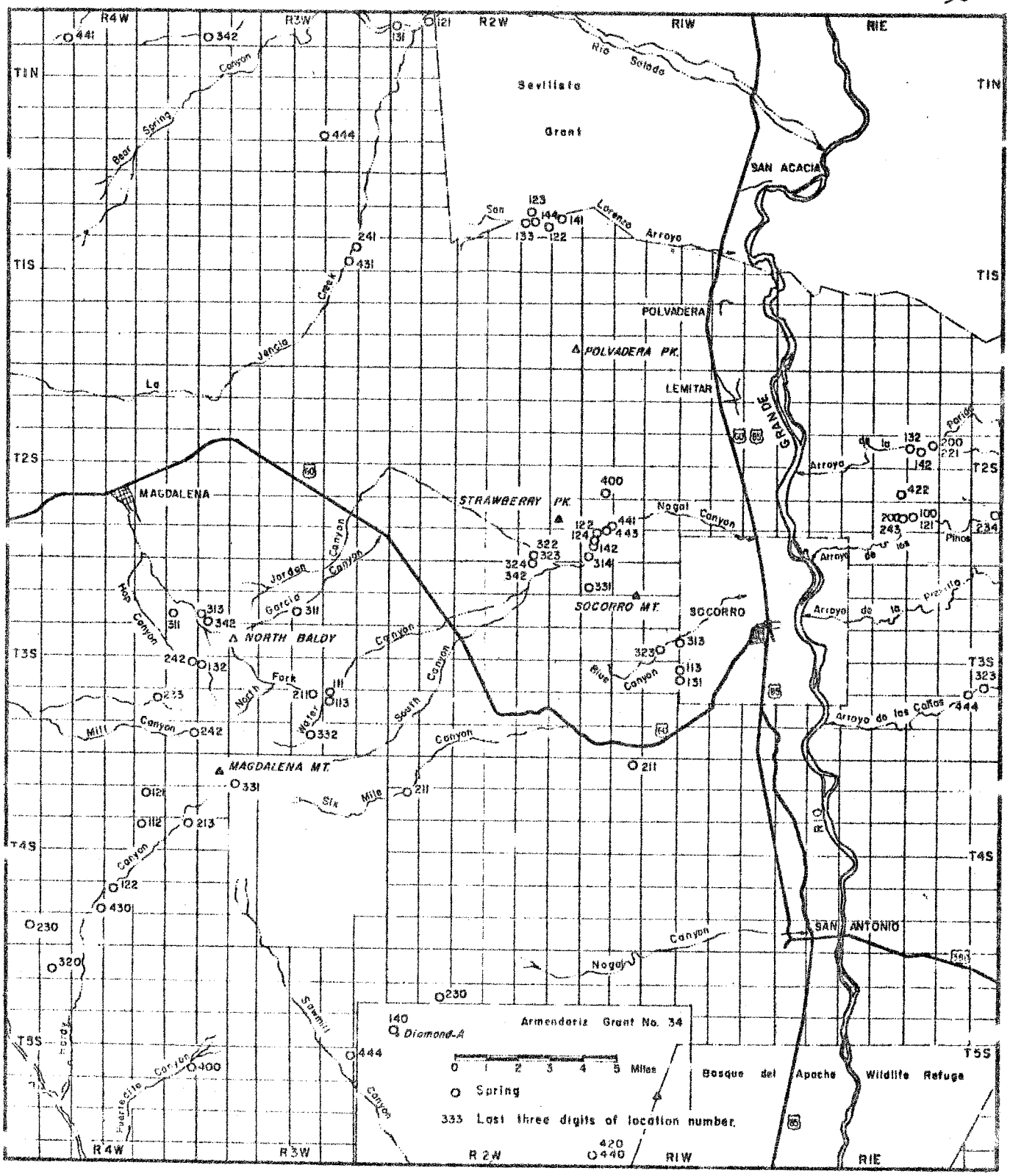

Figure 21. Springs in the Socorro region, New Mexico, (Hall, 1963).

restricted in areal extent, and (3) the travel time from recharge to discharge area (~ 16-17 km) was measured to be about four years, which indicates very fast water movement (~ 11 meters/day) (Holmes, 1963). If the travel time of the water is accurate and the recharge area correctly located, the water must travel at shallow depths ($\leq$ 2 km). Thus, the percentage of the raypaths, considering the depths of the events (4-9 km), which travels through ground water-filled cracks would be too small to induce the high observed Poisson's ratios.

Pressure-Temperature

Pressure and temperature will be discussed together because some investigators, Crosson and Christiansen (1967) and Fagerne and Kanestrom (1973), believe that Poisson's ratio is independent of pressure and temperature.

Pressure-temperature data from two papers by Hughes and Maurette (1956, 1957) are presented in Tables 6 and 7. Their pressure-temperature studies on granites and other igneous rocks corresponded to pressures up to about 7 kb and temperatures to 400°C. For rocks of the same composition in Tables 6 and 7, the effects of temperature and pressure are only slight. Increases in pressure and temperature seem to offset one another because little or no correlation between Poisson's ratio and depth is apparent. One cannot be sure, however, that the laboratory can truly duplicate the conditions in the earth.

Composition

The data of Hughes and Maurette (1957) listed in Table

Table 6. Pressure-Temperature Data on Granites (Hughes and Maurette, 1956).

Depth (km)		1	2	5	10	15
Temperature (°C.)		45	70	135	225	290
Pressure (bars)		260	520	1,300	2,600	3,900
Texas Gray	V_D	5.90	6.00	6.02	6.02	6.01
	V_R	3.45	3.55	3.57	3.57	3.57
	σ	.240	.231	.229	.229	.227
Texas Pink	V_D	6.08	6.24	6.32	6.30	6.27
	V_R	3.39	3.32	3.32	3.32	
	σ	.293	.303	.309	.308	
Woodbury	V_D	5.90	6.05	6.15	6.14	6.04
	V_R	3.34	3.43	3.54	3.61	
	σ	.264	.263	.252	.236	

Table 7. Pressure-Temperature Data on Selected Igneous Rocks (Hughes and Maurette, 1957).

Depth (km)		1	2	5	10	15	20	25
Temperature °C.		45	70	135	225	290	350	400
Pressure (bars)		260	520	1,300	2,600	3,900	5,300	6,700
San Marcos Gabbro	V_D	6.70	6.79	6.90	6.96	6.95	6.8	6.80
	V_R	3.47	3.49	3.51	3.52	3.51	3.47	3.44
	σ	.317	.320	.325	.328	.329	.329	.328
Bytownite Gabbro	V_D	6.50	6.56	6.60	6.57	6.53		
	V_R	3.41	3.42	3.42	3.44	3.43		
	σ	.310	.313	.316	.311	.309		
Hornblende Gabbro	V_D	6.60	6.65	6.71	6.74	6.75		
	V_R	3.57	3.60	3.64	3.69	3.68		
	σ	.293	.293	.291	.286	.289		
Analcime	V_D	5.41	5.45	5.51	5.59	5.62		
	V_R	3.05	3.06	3.07	3.07	3.05		
	σ	.267	.270	.275	.284	.291		
Basalt	V_D	5.44	5.58	5.68	5.74	5.79		
	V_R	3.21	3.21	3.22	3.23	3.23		
	σ	.233	.253	.263	.269	.274		
Dunite	V_D	7.35	7.46	7.50	7.22			
	V_R	3.77	3.85	3.90	3.68			
	σ	.321	.319	.315	.324			

7 shows that Poisson's ratio is dependent on composition. Note again that for most of the igneous rocks, Poisson's ratio changes only slightly with increase in pressure and temperature to maximums of 7 kb and 300°C.

The San Marcos Gabbro and Dunite in Table 7 have a Poisson's ratio of 0.32. If rocks, whose physical properties corresponded closely to the aforementioned rocks, were located in the local Socorro area, one might expect a higher than normal Poisson's ratio along some increments of the microearthquake raypaths. The composition of Precambrian rocks most likely to underlie the Socorro region are given in Table 8. These rocks are not similar in composition to the San Marcos Gabbro and Dunite in Table 7. For comparison purposes, velocities and Poisson's ratios for the Socorro Precambrian rocks were determined in two ways: (1) from the bulk velocities of these rocks (Clark, 1966) and (2) from the velocities of the individual mineral constituents (Table 9). The results are shown in Table 8. As can be seen from the table, the most likely Precambrian rocks in the Socorro area could not produce the Poisson's ratio anomalies found from the raypath technique. One could argue that some unknown volume of gabbro lies beneath Socorro, but to produce the observed anomalies, the raypaths would have to travel through predominantly gabbro, which geologically, is not realistic in the Socorro area (Budding, 1976).

Table 8. Physical Parameters of the Precambrian Rocks near Socorro, N.M.

ROCK	LOCATION	DENSITY	PRESSURE	Vp km/sec	Vs km/sec	POISSON'S RATIO	* REF.
QTZ.MONZ.	PORTERVILLE,CA.	2.664	1kb	5.95	3.63	.204	1
HORNBLENDE GABBRO	ESCONDIDO,CA.	-	.2kb	6.60	3.56	.295	1
QTZ.MONZ.	EAST OF RIO GRANDE, SOCORRO, N.M.	2.66	ATMOS.	6.03	3.57	.231	2,3
QTZ.MONZ.	OSCURA MTS.,N.M.	2.67	ATMOS.	6.05	3.57	.233	2,3
GRANITE-GNEISSES	LA JOYITA HILLS N.M.	2.67	ATMOS.	5.98	3.53	.233	2,3
QTZ.MONZ.	LADRON MTS., N.M.	2.64	ATMOS.	6.09	3.53	.246	2,3
HORNBLENDE GABBRO	MAGDALENA MTS., N.M.	-	ATMOS.	6.81	3.67	.295	2,3

*Numbers in this column are for the references listed below:

1 GSA Memoir 97, ed. Clark (1966)

2 Budding (1976)

3 Christiansen and Fountain (1975)

Table 9. Mineral Percentages in the Precambrian Rocks near Socorro, N.M., (Budding, 1976).

ROCK	LOCATION	QTZ	MICROCLINE	PLAG.AN_{25}	PLAG.AN_{40}	BIOT.	MUSC.	MAGNET.	HORN.
QTZ. MONZ.	EAST OF RIO GRANDE SOCORRO, N.M.	32	34	25	0	4	4	1	0
QTZ. MONZ.	OSCURA MTS., N.M.	31	31	30	0	5	2	1	0
GRAN. GNEIS.	LA JOYITA MTS.N.M.	30	45	13	0	10	1	1	0
QTZ. MONZ.	LADRON MTS.N.M.	23	45	30	0	1	0	1	0
HORN. GAB- BRO	MAGDA- LENA,MTS. N.M.	0	0	0	50	0	0	0	50

Change of Vs in the Socorro Area

Assuming that Poisson's ratio is 0.26 in the Socorro area, then the corresponding Vp/Vs ratio is 1.756. This velocity ratio is interesting if one considers the results obtained by Kiet Sakdejayont (1974). He found the Vp/Vs ratio to be 1.664 for the area between Socorro and Albuquerque. It should be noted that his velocity ratio is more dependent on the properties of the crust north of Bernardo to Albuquerque than the properties of the crust south of Bernardo to Socorro. Assuming a Vp of 5.8 km/sec for the Socorro area as well as the area north to Albuquerque, then a drop in Vs is indicated from a 3.49 km/sec in the rift to a 3.30 km/sec in the Socorro region or about a 5 percent reduction.

Several arguments can be made to explain the increase in Poisson's ratio and/or decrease in Vs in the Socorro area. First, the assumption that the Vp is the same in the Socorro area and north to Albuquerque may be incorrect. There are, however, several measurements which substantiate a Vp of 5.8 km/sec in both regions. Toppozada (1974) and Toppozada and Sanford (1976) have found good evidence for a Vp of 5.8 km/sec between Socorro and Albuquerque as well as the local Socorro area.

Another argument is that the geothermal gradient in the Socorro region is much greater than other areas in the

Rio Grande Rift. Heat flow measured in the Socorro region is significantly higher than other areas of the rift (Sanford and Reiter, paper in preparation). The increased temperatures affect the shear modulus much more than the bulk modulus, so that a decrease in Vs might be expected (Walsh, 1969). If the higher geothermal gradient truly exists, one might expect a partial or full melt in areas where effective pressure is small and water is abundant.

The Change in Vp, Vs, and ν with a Changing Shear Modulus

J.B. Walsh in a 1969 publication concluded that a rather large decrease in rigidity can be expected in partially melted regions, but with only a small decrease in the bulk modulus. Using the following equations:

K= Bulk Modulus= $\rho(Vp^2-4/3Vs^2)$
μ= Shear Modulus= ρVs^2
ρ = Density, assumed 2.67g/cc
ν= Poisson's ratio= $((Vp/Vs)^2-2)/2((Vp/Vs)^2-1)$
Vp= P-wave velocity
Vs= S-wave velocity

and Walsh's conclusion that the bulk modulus is little affected, one can calculate the changes in Vp, Vs, and with a change in the shear modulus (Table 10).

The analysis indicates that decreases in the shear modulus will reduce Vs by a factor of two over Vp. Also, by reducing the shear modulus for the Socorro region by 36 percent, a 29 percent increase in Poisson's ratio occurs. So, moderate changes in the shear modulus produces relatively large changes in Poisson's ratio. These results can be supported by a Spetzler and Anderson (1968) publication which showed that a sudden increase in attenuation and a decrease in Vs will occur when melting begins even though the melt concentration may be minute.

Attenuation and S-wave screening, observations characteristic of a reduced shear modulus, have been noted

Table 10. The Changes in Vp, Vs, and with a Changing Shear Modulus.

$X10^{11}$ cgs	%Change from initial value	Vp km/sec	%Change from initial value	Vs km/sec	%Change from initial value		%Change from initial value	K $X10^{11}$ cgs
2.908	0	5.80	0	3.30	0	.261	0	5.105
2.624	9.8	5.68	2.1	3.14	5	.281	7.1	5.105
2.355	19.0	5.56	4.1	2.97	10	.300	14.9	5.105
2.101	27.8	5.44	6.2	2.81	15	.319	22.2	5.105
1.861	36.0	5.33	8.1	2.64	20	.337	29.1	5.105
1.000	65.6	4.91	15.3	1.94	41.4	.408	56.3	5.105

and studied in the Socorro region (Shuleski, 1976). These observations support the most important conclusion of this study, that the Poisson's ratio anomalies defined earlier by the raypath technique can be explained by one or more shallow partial melts.

Geothermal Potential

The geothermal potential of the Socorro area has been downgraded by some. It is argued that the thermal springs are only warm (90-91°F) and could be heated by some other means than a recent intrusive. In considering this argument, let's discuss the two types of known geothermal fields: (1) the thermal area which yields dry or slightly superheated steam and (2) the thermal area which produces saturated steam and hot water. The principal factors which give rise to these two types of geothermal fields are: (1) the initial heat content of the thermal fluid, which is determined by the temperature of the heat source and (2) the amount by which the thermal fluid is diluted by cold ground water. This second factor is controlled principally by the structure and permeability of the rocks overlying the heat source. Assuming an intrusive is located in a structural depression, like the La Jencia Basin, the ascending thermal fluid will mix with the cold ground water. The above conditions would probably result in a thermal area which yields only warm water. This might explain the warm temperatures of the Socorro Spring. Therefore, the presence of warm instead of hot springs may not necessarily reflect the true geothermal potential of the region.

Of the many factors that affect the geothermal

resource estimates for the Socorro area, four are of significance: (1) reservoir volume, (2) recoverability, (3) temperature, and (4) technology and economics of use. It is unfortunate that the study of Poisson's ratio cannot be used to study any of these factors at this time. The above factors must be investigated by refined geophysical techniques or by some deep drilling in a suspected thermal area. But one area in the investigation of geothermal resources in which the study of Poisson's ratio might be useful is indicating those areas which could have magma present.

Acknowledgements

The author wishes to thank Dr. Allan R. Sanford for his advise in all aspects of the research. Rick Mott, Eric Rinehart, Paul Shuleski, Terry Wallace, and Roger Ward are extended a gracious thanks for their efforts in data acquisition. The author is particularly thankful to Rick Mott and Eric Rinehart for their work in locating the microearthquakes used in this study, to Terry Wallace for his help in computer-related problems, and to Pat Buckley for his statistical expertise. Particular appreciation must be extended to the author's wife for her patience and understanding.

Appendix I

Data Listing

DATE	ITER.O.T.	LAT.	LONG	DEPTH	P ARRIVALS	S-P	GRADE	STAT	SLOPE	ST.DEV.SLOPE	WAD.O.T.	POIS.RA
5-22-75	11:36:29.03	33.9397	106.9395	4.70	31.95	2.41	E	SC	.7538	.0506	11:36:28.86	.259
					32.64	2.98	E	EM				
					33.06	3.08	G	CC				
					29.91	0.80	E	CM				
					31.79	2.09	E	CT				
5-22-75	13:19:41.40	33.9503	106.9430	99.99	45.20	3.01	E	CC	.7703	.0216	13:19:41.35	.266
					42.29	0.76	E	CM				
					44.51	2.41	G	SC				
					45.03	2.85	P	EM				
					43.96	1.95	P	CT				
6- 3-75	15:10:15.60	34.0301	107.0296	9.50	18.43	2.25	G	CC	.7894	.0629	15:10:15.61	.273
					17.53	1.50	E	SC				
					18.10	2.10	G	CM				
					17.84	1.65	P	CT				
					19.66	3.16	E	EM				
7-30-75	21:44:42.10	34.0848	106.9223	8.20	43.61	1.15	E	WT	.7701	.0385	21:44:42.08	.266
					45.11	2.43	E	CM				
					44.58	1.90	E	EM				
					44.18	1.65	G	CC				
					45.53	2.60	G	SC				
8- 5-75	2:26: 2.50	34.0335	106.9772	7.60	4.06	1.35	E	WT	.7621	.0366	2:26: 2.29	.262
					4.84	2.00	G	SC				
					5.70	2.60	E	EM				
					4.63	1.75	G	CM				
					5.03	2.05	G	CC				
8- 5-75	4:17:20.92	34.0379	106.9758	7.80	23.36	2.00	E	CC	.8214	.0736	4:17:21.00	.284
					22.50	1.15	E	WT				
					23.20	1.80	E	SC				
					24.19	2.55	E	EM				
					23.08	1.70	E	CM				
8- 8-75	10:53:58.30	34.0837	106.9233	6.70	0.90	2.40	E	CM	.7880	.0269	10:53:57.93	.272
					0.14	1.75	E	EM				
					59.96	1.60	P	CC				
					59.14	0.95	E	WT				
					1.16	2.50	E	SC				
8- 8-75	10:57:22.59	34.0796	106.9329	6.80	25.31	2.45	E	CM	.7998	.0428	10:57:22.36	.277
					24.80	1.90	E	EM				
					24.34	1.55	E	CC				
					25.54	2.50	E	SC				
					23.52	0.65	E	WT				
8-12-75	7: 9:11.15	34.0357	106.8225	0.0	13.16	1.99	E	WT	.7318	.0625	7: 9:10.57	.253
					13.84	2.56	G	CM				
					14.44	2.86	G	CC				
					13.60	2.30	G	MY				
					12.06	0.90	E	EM				
					15.52	3.46	E	SC				
8-12-75	15:25:28.30	34.0513	106.9785	8.80	33.35	3.76	E	MY	.9565	.1053	15:25:28.95	.323
					30.67	1.60	E	CC				
					30.78	1.65	E	SC				
					29.94	1.05	E	WT				
					31.51	2.56	E	EM				
					30.81	1.70	E	CM				
8-13-75	5:19:18.20	34.0823	106.9237	7.30	20.35	1.60	G	CC	.7432	.0356	5:19:18.18	.255
					21.20	2.36	G	CM				
					20.64	1.81	E	EM				
					21.60	2.58	E	SC				
					19.67	1.10	E	WT				
					21.82	2.66	P	MY				
8-13-75	7:39:18.40	34.0826	106.9274	7.90	22.02	2.81	E	MY	.7781	.0382	7:39:18.51	.269
					20.51	1.50	E	CC				
					21.46	2.25	E	CM				
					19.82	1.10	E	WT				
					20.88	1.80	E	EM				
					21.73	2.51	E	SC				
8-13-75	11:22:26.90	34.0245	106.9731	9.10	29.37	2.00	E	SC	.7402	.0397	11:22:26.69	.253
					30.21	2.56	E	EM				
					28.76	1.50	E	WT				
					28.93	1.65	E	CM				
					29.59	2.20	E	CC				
8-20-75	5:16:39.70	34.0882	106.9261	10.10	43.57	2.79	E	SC	.7061	.0316	5:16:39.69	.238
					43.34	2.52	P	EM				
					42.39	1.90	E	EM				
					42.61	2.05	P	CC				
					41.79	1.50	P	WT				
8-20-75	15:29:36.60	34.0848	106.9261	6.90	39.52	2.25	E	CM	.7271	.0439	15:29:36.47	.248
					40.82	3.11	E	SC				
					38.69	1.90	E	EM				
					38.50	1.43	E	CC				
					37.86	0.95	E	WT				
8-20-75	12:20:52.35	34.0833	106.9153	7.00	56.56	2.51	E	SC	.8255	.0520	12:20:52.56	.286
					54.27	1.45	G	CC				
					55.22	2.10	G	EM				

13-75	11:22:26.90	34.0245	106.9731	9.10	20.51	1.50	E	CC					
					21.46	2.25	E	CM					
					19.82	1.10	G	WT					
					20.88	1.80	G	FM					
					21.73	2.51	G	SC					
					29.37	2.00	G	SC	.7402	.0397	11:22:26.69	.253	
					30.21	2.56	G	FM					
					28.76	1.50	G	WT					
					28.93	1.65	G	CM					
20-75	5:16:39.70	34.0882	106.9261	10.10	29.59	2.20	G	CC					
					43.57	2.79	E	SC	.7061	.0316	5:16:39.69	.238	
					43.34	2.52	E	CM					
					42.39	1.90	E	FM					
					42.61	2.05	E	CC					
20-75	15:29:36.60	34.0848	106.9261	6.90	41.79	1.50	E	WT					
					39.52	2.25	E	CM	.7271	.0439	15:29:36.47	.248	
					40.82	3.11	E	SC					
					38.89	1.90	E	FM					
					38.50	1.43	E	CC					
20-75	12:20:52.35	34.0833	106.9153	7.00	37.86	0.95	E	WT					
					55.56	2.51	E	SC	.8255	.0520	12:20:52.56	.286	
					54.27	1.45	E	CC					
					55.22	2.10	E	CM					
					53.60	0.80	E	WT					
					54.29	1.50	E	FM					
21-75	3:44:48.70	34.0407	107.0470	9.50	51.37	2.15	E	CC	.7671	.0658	3:44:48.79	.264	
					51.14	1.70	E	WT					
					50.63	1.38	E	SC					
					51.40	2.00	E	CM					
					53.01	3.21	E	FM					
21-75	19: 4: 6.50	34.0575	106.9692	7.50	8.62	1.75	E	CC	.7891	.0723	19: 4: 6.38	.273	
					9.03	2.00	E	SC					
					8.89	2.10	E	CM					
					9.56	2.51	E	FM					
					7.91	1.20	E	WT					
29-75	8:52:18.80	34.0737	106.9271	7.20	20.06	1.10	G	WT	.8032	.0592	8:52:18.79	.278	
					21.55	2.20	E	CM					
					20.82	1.55	G	CC					
					21.94	2.61	G	SC					
					21.09	1.80	G	FM					
16-75	13:30:52.55	34.0804	106.9301	6.70	57.56	3.76	P	HC	.7049	.0165	13:30:52.26	.238	
					55.34	2.25	E	CM					
					57.73	3.81	P	MG					
					57.73	3.86	P	NJ					
					53.74	1.00	E	WT					
4-75	16:30:12.10	34.0491	107.0517	10.00	17.60	4.00	G	MY	.6236	.0169	16:30:11.16	.194	
					14.12	1.85	G	WT					
					14.72	2.30	E	CM					
					13.55	1.45	E	SC					
					14.47	2.05	E	CC					
5-75	22:28:26.70	34.0424	107.0228	4.50	28.28	1.55	E	WT	.9144	.0223	22:28:26.65	.312	
					28.94	2.01	E	CC					
					28.98	2.10	E	CM					
					28.26	1.50	E	SC					
					31.78	4.71	P	MY					
7-75	8:27:36.10	34.0480	107.0323	7.10	38.54	1.85	E	CC	.6652	.0607	8:27:35.55	.218	
					42.83	4.61	P	NJ					
					38.60	2.10	G	CM					
					38.03	1.60	G	WT					
					41.34	4.19	P	MY					
27-76	8:37:44.73	34.1290	106.8220	8.90	49.38	3.71	P	CM	.7961	.0526	8:37:44.75	.275	
					46.34	1.20	E	DM					
					47.05	1.70	E	TA					
					47.46	2.35	E	WT					
					50.05	4.16	G	SC					
					47.77	2.46	G	CC					
27-76	10: 5:24.07	34.1490	106.8060	9.60	25.97	1.40	G	DM	.7207	.0163	10: 5:24.01	.245	
					27.16	2.30	E	WT					
					29.67	4.06	E	SC					
					27.35	2.46	G	CC					
					26.64	1.85	G	TA					
					28.99	4.41	P	CM					
29-76	15: 6:40.70	34.0000	106.9680	6.50	44.03	3.00	P	DM	.7793	.0587	15: 6:40.38	.269	
					42.23	1.50	E	WT					
					43.96	2.70	E	TA					
					42.74	1.70	G	SC					
					43.30	2.25	G	CC					
					41.80	1.15	G	CM					
17-76	6:17:49.07	34.0450	107.0620	10.20	52.06	2.25	P	CM	.7364	.0768	6:17:49.05	.252	
					51.20	1.65	E	WM					
					51.63	1.85	E	WT					
					51.37	1.65	E	IC					
					51.03	1.45	E	SC					
17-76	17:34: 5.13	34.0520	107.0040	8.20	7.14	1.30	E	WM	.8942	.1464	17:34: 5.66	.307	
					7.21	1.30	E	WT					
					7.91	2.00	E	CM					
					7.35	1.65	E	IC					
					7.71	1.80	E	CC					
18-76	23:25:35.22	34.0420	107.0520	6.20	37.78	1.85	G	WT	.6623	.0317	23:25:34.95	.216	
					37.53	1.75	G	IC					
					37.16	1.45	G	SC					
					37.36	1.60	G	WM					
					38.23	2.20	G	CM					
					38.24	2.15	G	CC					
19-76	0: 8:36.77	34.0260	107.0610	8.60	39.55	2.20	G	CM	.7363	.0926	0: 8:36.78	.252	
					38.66	1.40	G	SC					
					38.93	1.55	G	WM					
					39.87	2.20	G	CC					
					38.87	1.55	G	IC					
					39.38	1.85	G	WT					
20-76	12:51:45.10	34.0310	107.0450	99.99	47.88	2.00	G	CM	.8091	.1246	12:51:45.43	.280	
					47.29	1.45	E	SC					
					47.65	1.75	E	WT					
					47.34	1.55	E	WM					
					47.30	1.60	E	IC					
18-76	14:45:16.00	33.9760	106.7260	99.99	18.54	1.71	P	TA	.7531	.0432	14:45:16.37	.259	
					19.37	2.11	P	DM					
					20.40	3.11	P	WT					
					20.48	3.06	P	CM					
					20.80	3.36	P	IC					
					18.69	1.76	P	FR					
18-76	18:34:51.00	34.0420	107.0750	6.10	53.00	1.61	E	IC	.6567	.0415	18:34:50.53	.213	
					53.76	2.20	G	CM					
					53.38	1.81	G	WT					
					55.48	3.36	G	DM					
					55.81	3.36	G	TA					
23-76	12:53:20.55	34.2500	106.8370	99.99	26.39	4.67	P	IC	.5576	.0760	12:53:17.80	.149	
					24.79	4.01	P	TA					
					24.79	4.21	P	WT					
					28.20	5.77	P	FR					
					23.80	3.06	G	DM					
25-76	10:50:54.65	34.0425	106.9435	5.50	56.30	1.61	E	IC	.8387	.0177	10:50:54.32	.290	
					55.77	1.21	E	WT					
					57.34	2.56	G	DM					
					56.76	2.11	G	CM					
					59.43	4.27	G	FR					
13-76	9:45:40.73	34.0720	107.0050	6.10	43.34	2.11	E	CM	.8005	.0543	9:45:40.71	.277	
					43.77	1.71	E	SC					

					20.40	3.11	P	WT			
					20.48	3.05	P	CM			
					20.80	3.36	E	IC			
					18.69	1.76	P	FR			
18-76	18:34:51.00	34.0420	107.0750	6.10	53.00	1.61	E	IC	.6567	.0415	18:34:50.53	.213
					53.76	2.20	G	CM			
					53.38	1.81	G	WT			
					55.48	3.36	G	DM			
					55.81	3.36	P	TA			
23-76	12:53:20.55	34.2500	106.8370	99.99	26.39	4.67	P	IC	.5576	.0760	12:53:17.80	.149
					24.79	4.01	P	TA			
					24.79	4.21	G	WT			
					28.20	5.77	P	FR			
					23.80	3.06	G	DM			
25-76	10:50:54.65	34.0425	106.9435	5.50	56.30	1.61	E	IC	.8387	.0177	10:50:54.32	.290
					55.77	1.21	G	WT			
					57.34	2.56	G	DM			
					56.76	2.11	G	CM			
					59.43	4.27	G	FR			
13-76	9:45:40.73	34.0720	107.0050	6.10	43.34	2.11	E	CM	.8005	.0543	9:45:40.71	.277
					42.77	1.71	E	SC			
					42.03	1.10	E	WT			
					42.52	1.46	E	CC			
					42.68	1.51	E	IC			
					42.39	1.31	E	WM			
13-76	11:41:25.73	34.0450	107.0540	11.40	28.42	2.25	E	CM	.7053	.1008	11:41:25.30	.238
					27.37	1.41	G	SC			
					27.97	1.86	G	WT			
					28.31	2.11	E	CC			
					27.74	1.61	P	IC			
					27.45	1.66	P	WM			
13-76	11:58:34.65	33.9900	106.9510	6.40	36.08	1.05	G	WM	.6893	.0232	11:58:34.52	.233
					35.95	0.95	G	IC			
					37.85	2.26	E	CC			
					36.57	1.46	G	WT			
					37.18	1.86	E	SC			
					36.02	1.05	G	CM			
13-76	23:15:15.00	34.0300	107.0250	6.00	16.46	1.15	E	SC	.7256	.0447	23:15:14.93	.247
					17.33	1.76	E	CC			
					16.23	0.95	P	IC			
					16.75	1.26	G	WT			
					16.11	0.85	G	WM			
14-76	1:50:28.91	33.9910	106.9950	9.10	30.74	1.36	E	WM	.6584	.2088	1:50:28.44	.214
					31.48	1.81	E	WT			
					30.63	1.31	E	IC			
					30.91	2.11	P	CM			
					32.25	2.56	E	CC			
					31.34	1.86	E	SC			
14-76	13:12:21.50	34.0710	107.0310	99.99	22.83	1.28	E	WM	.8331	.0835	13:12:21.28	.288
					23.08	1.61	G	IC			
					23.04	1.41	E	CC			
					23.89	2.16	P	CM			
					22.82	1.26	P	WT			
15-76	8:45:52.70	34.0630	107.0080	3.60	54.40	1.31	E	WM	.8943	.0327	8:45:52.92	.307
					54.60	1.46	G	CC			
					55.34	2.16	P	CM			
					54.65	1.56	G	IC			
					54.79	1.71	G	SC			
					54.16	1.10	P	WT			
15-76	18:28:37.46	34.0521	106.9574	4.80	38.62	1.00	G	WT	.8179	.0396	18:28:37.36	.283
					39.99	2.16	E	SC			
					39.17	1.51	G	IC			
					39.72	1.68	P	CM			
					39.04	1.41	P	WM			
16-76	5:34:38.85	34.0380	107.0230	6.10	40.11	0.90	G	WM	.9653	.0540	5:34:39.22	.325
					41.09	1.81	P	CM			
					40.31	1.00	P	IC			
					40.56	1.31	G	WT			
					40.46	1.21	E	SC			
16-76	9:33:43.03	34.0670	107.0070	6.60	44.86	1.51	E	CC	.8394	.0641	9:33:43.13	.290
					45.06	1.67	E	SC			
					44.45	1.06	E	WT			
					44.89	1.51	E	IC			
					45.59	2.00	E	CM			
					44.48	1.10	E	WM			
16-76	14: 7:33.47	34.0686	107.0067	6.90	35.50	1.70	E	SC	.9451	.1004	14: 7:33.82	.320
					35.34	1.33	P	CC			
					35.06	1.15	P	WM			
					36.07	2.10	E	CM			
					34.85	1.00	P	WT			
					35.41	1.55	P	IC			
20-76	2:52:19.33	34.0470	107.0620	99.99	23.89	3.31	E	DM	.6890	.0094	2:52:19.09	.233
					22.12	2.11	E	CC			
					23.28	2.91	P	SL			
					24.72	3.87	P	CU			
					21.75	1.81	E	WT			
20-76	8:32:19.19	34.0980	106.8430	4.00	21.40	1.81	E	BG	.6712	.0712	8:32:18.76	.221
					20.79	1.46	P	CU			
					22.74	2.56	E	SL			
					21.57	2.01	G	CC			
					20.09	0.75	E	DM			
21-76	11:16:20.17	34.2880	106.8530	99.99	24.40	4.17	P	WT	.8508	.1332	11:16:19.81	.294
					23.61	3.01	G	DM			
					22.71	2.71	E	CU			
					22.63	2.16	E	SL			
					21.76	1.81	P	BG			
					23.34	2.81	G	CC			
23-76	5:57:59.97	34.0600	107.0390	99.99	1.79	1.86	E	WT	.8027	.0598	5:57:59.56	.278
					3.34	2.86	E	SL			
					2.14	2.11	E	CC			
					3.90	3.41	P	DM			
					4.70	4.27	E	BG			

STOP 0

00:00:14

Avg 0.262

Appendix II

Wadati Origin Time 95 Percent Confidence Intervals

Using linear regression you assume that: $Y = a+bx_0$ is distributed $\sim N(0,\sigma^2)$ for the point of intercept with the x-axis. If we know σ^2, which we don't, then it would be a simple matter to calculate a confidence interval for x_0.

Since we don't know the true mean or variance, we have to resort to what is known as the "t" statistic. The "t" statistic is written as a ratio

$$t = \frac{\mu\sqrt{\gamma}}{\sqrt{v}}$$

where μ = standard N(0,1) random variable,
v^2 = a "x^2" random variable,
γ = degrees of freedom of v.

It can be shown that for sampling from a normal distribution that the quantity

$$t = \frac{\sqrt{N}(\bar{x}-\mu_0)\sqrt{N-1}}{\sqrt{\Sigma(x_i-\bar{x})^2}}$$ is such a ratio.

This can then be used to make statements concerning μ_0, the true mean. In our case from regression theory, we know that $a+bx_0 \sim N(0, \sigma_y^2)$

where $$\sigma_y^2 = \sigma^2\left[1/N + \frac{(x_0-\bar{x})^2}{S_{xx}}\right]$$

$$S_{xx} = \sum^{N}(x_i-\bar{x})^2$$

Specifically, this tells us that

$$\frac{a+bx_0}{\sqrt{\sigma^2\left[1/N + \frac{(x_0-\bar{x})^2}{S_{xx}}\right]}}$$

is a standard N(0,1) random variable.

Regression theory also states that

$$(N-2)\frac{\hat{\sigma}^2}{\sigma^2} \text{ is a "}x^2\text{" random variable}$$

with N-2 degrees of freedom. Hence, we form the "t" random variable by

$$\text{"t"} = \frac{a+bx_0}{\sigma\left[1/N + \frac{(x_0-\bar{x})^2}{S_{xx}}\right]^{1/2}} \frac{\sqrt{N-2}\,\hat{\sigma}}{\sigma\sqrt{N-2}}$$

$$\text{"t"} = \frac{a+bx_0}{S\left[1/N + \frac{(x_0-\bar{x})^2}{S_{xx}}\right]^{1/2}}$$

where

$$s^2 = \hat{\sigma}^2 = 1/N-2\left[\Sigma(Y_i-\bar{Y})^2 - \frac{(\Sigma(x_i-\bar{x})(Y_i-\bar{Y}))^2}{\Sigma(x_i-\bar{x})^2}\right]$$

The value of this is that we know what the "t" distribution is so we can make confidence statements concerning x_0. Hence,

$$(a+bx_0)^2 \le t^2_{\alpha/2} S^2\left[1/N + \frac{(x_0-\bar{x})^2}{S_{xx}}\right] \text{ with}$$

probability $1-\alpha$. So,

$$a^2 + 2abx_0 + b^2x_0 \le t^2_{\alpha/2} S^2\left[1/N + \frac{x_0^2 - 2\bar{x}x_0 + \bar{x}^2}{S_{xx}}\right] \text{with}$$

probability 1-x. Also, $\left[b^2 - \frac{t^2_{\alpha/2}S^2}{S_{xx}}\right]x_0^2 + 2\left[a+b+\frac{t^2\bar{x}s^2}{S_{xx}}\right]x_0 + \left[a^2+t^2+S^2\left(1/N+\frac{\bar{x}^2}{S_{xx}}\right)\right] \le 0$ with probability $1-\alpha$. Solving this equation for x_0 gives two values, x_1 and x_2. The $1-\alpha$ confidence interval for x_0 is (x_1, x_2).

<u>95 Percent Confidence Interval on the Slope and</u>

Assuming $a+bx_0$ is distributed normal $(0, \sigma y_0^2)$. The var$(a+bx_0)$ equals

$$\sigma^2\left[1/N + \frac{(x_0-\bar{x})^2}{S_{xx}}\right].$$

Also, $S^2 = \frac{1}{N-2}\left[\Sigma(Y_i-\bar{Y})^2 - \frac{[\Sigma(x_i-\bar{x})(Y_i-\bar{Y})]^2}{\Sigma(x_i-\bar{x})^2}\right]$

$$t_{\alpha/2} = \begin{cases} 2.571 & n=5 \\ 2.447 & n=6 \end{cases} \quad \alpha\ .05$$

$$\nu = \text{Poisson's Ratio} = \frac{(b+1)^2-2}{2(b+1)^2-2}$$

$$b \sim N(\hat{b}, c_{ii}\sigma^2)$$

Use the regression program to get the standard deviation on the slope and call this g. Then

$$P\left[-t_{\alpha/2} \leq \frac{\hat{b}-b}{g} \leq t_{\alpha/2}\right] = 1-\alpha = 0.95$$

$$P\left[-g t_{\alpha/2} \leq \hat{b}-b \leq t_{\alpha/2}\, g\right] = 0.95$$

$(\hat{b} - g t_{\alpha/2}, \hat{b} + g t_{\alpha_2})$ is the 95 percent confidence interval on the slope. Plug in values to get (γ_1, γ_2), the 95 percent confidence interval for where

$$g = \sqrt{s^2\left[\frac{1}{\Sigma(x_i-\bar{x})^2}\right.}$$

Appendix III

Socorro Raypath Analysis Using Iterative Origin Times

```
STA=CM  LAT= 33.9501  LONG=106.9579
BL= 0.798205  B= 0.892137  BH= 0.986069
POISL=0.276140  POIS=0.306215  POISH=0.330190
D=  0.  E= 10.
DATA POINTS=  5

BL= 0.734014  B= 0.766644  BH= 0.799274
POISL=0.250847  POIS=0.264265  POISH=0.276525
D= 10.  E= 20.
DATA POINTS= 10

BL= 0.722444  B= 0.760226  BH= 0.798008
POISL=0.245781  POIS=0.261722  POISH=0.276069
D=310.  E=320.
DATA POINTS=  7

BL= 0.789757  B= 0.873808  BH= 0.957858
POISL=0.273060  POIS=0.300888  POISH=0.323522
D=320.  E=330.
DATA POINTS=  6

BL= 0.674325  B= 0.839823  BH= 1.005322
POISL=0.222740  POIS=0.290352  POISH=0.334509
D=330.  E=340.
DATA POINTS=  4

BL= 0.751370  B= 0.787809  BH= 0.824248
POISL=0.258138  POIS=0.272340  POISH=0.285212
D=340.  E=350.
DATA POINTS=  9

BL= 0.765284  B= 0.907817  BH= 1.050349
POISL=0.263730  POIS=0.313589  POISH=0.343942
D=350.  E=360.
DATA POINTS=  3


STA=CC  LAT= 34.1442  LONG=106.9812
BL= 0.716966  B= 0.759634  BH= 0.802301
POISL=0.243323  POIS=0.261485  POISH=0.277638
D=140.  E=150.
DATA POINTS=  9

BL= 0.732740  B= 0.773411  BH= 0.814083
POISL=0.250298  POIS=0.266898  POISH=0.281745
D=170.  E=180.
DATA POINTS=  9

BL= 0.728136  B= 0.773826  BH= 0.829516
POISL=0.248295  POIS=0.268970  POISH=0.296973
D=190.  E=200.
DATA POINTS=  9

BL= 0.692617  B= 0.779505  BH= 0.866392
POISL=0.231996  POIS=0.269227  POISH=0.298665
D=200.  E=210.
DATA POINTS=  7

BL= 0.735846  B= 0.807144  BH= 0.878442
POISL=0.251634  POIS=0.279324  POISH=0.302257
D=210.  E=220.
DATA POINTS=  4


STA=FM  LAT= 34.0829  LONG=106.8040
BL= 0.757959  B= 0.783149  BH= 0.808340
POISL=0.260813  POIS=0.270602  POISH=0.279744
D=250.  E=260.
DATA POINTS=  7

BL= 0.741213  B= 0.797739  BH= 0.854265
POISL=0.253915  POIS=0.275972  POISH=0.294939
D=260.  E=270.
DATA POINTS=  5

BL= 0.707444  B= 0.754889  BH= 0.802334
POISL=0.239953  POIS=0.259573  POISH=0.277620
D=270.  E=280.
DATA POINTS=  6
```

```
ATA POINTS=  3


TA=CU  LAT= 34.1573  LONG=106.7785


TA=SL  LAT= 34.0000  LONG=106.0000
L= 0.659492  B= 0.783871  BH= 0.908250
OISL=0.214923  POIS=0.270873  POISH=0.310708
=190.  E=200.
ATA POINTS=  3


TA=FR  LAT= 34.0000  LONG=106.0000


TA=BG  LAT= 34.2068  LONG=106.8205


TA=IC  LAT= 34.0000  LONG=106.0000
BL= 0.755645  B= 0.806242  BH= 0.856839
OISL=0.259879  POIS=0.279006  POISH=0.295739
)= 20.  E= 30.
ATA POINTS=  3

BL= 0.694738  B= 0.769917  BH= 0.845095
OISL=0.232825  POIS=0.265545  POISH=0.292046
)=300.  E=310.
ATA POINTS=  3

BL= 0.711006  B= 0.722113  BH= 0.733219
OISL=0.240602  POIS=0.245634  POISH=0.250505
)=310.  E=320.
ATA POINTS=  3

BL= 0.727907  B= 0.776284  BH= 0.824662
OISL=0.248194  POIS=0.269001  POISH=0.285352
)=320.  E=330.
ATA POINTS=  3

BL= 0.624297  B= 0.721224  BH= 0.818151
OISL=0.194813  POIS=0.245237  POISH=0.283143
)=330.  E=340.
ATA POINTS=  3

BL= 0.754703  B= 0.782782  BH= 0.810860
OISL=0.259497  POIS=0.270464  POISH=0.280626
)=350.  E=360.
ATA POINTS=  6


STA=WM  LAT= 34.0000  LONG=106.0000
BL= 0.638325  B= 0.731226  BH= 0.824127
OISL=0.203106  POIS=0.249642  POISH=0.285172
)=290.  E=300.
ATA POINTS=  3

BL= 0.661402  B= 0.823560  BH= 0.985717
OISL=0.215950  POIS=0.284980  POISH=0.330109
)=300.  E=310.
ATA POINTS=  4

BL= 0.647251  B= 0.714792  BH= 0.782333
OISL=0.208189  POIS=0.242336  POISH=0.270296
)=340.  E=350.
ATA POINTS=  5


STA=DM  LAT= 34.1075  LONG=106.8079
BL= 0.698513  B= 0.774222  BH= 0.849931
OISL=0.234740  POIS=0.267210  POISH=0.293579
)=250.  E=260.
ATA POINTS=  5


STA=SC  LAT= 34.0100  LONG=107.0894
BL= 0.551911  B= 0.831833  BH= 1.111754
OISL=0.144994  POIS=0.287741  POISH=0.355471
)= 30.  E= 40.
ATA POINTS=  3

BL= 0.752158  B= 0.801715  BH= 0.851271
OISL=0.258460  POIS=0.277399  POISH=0.294001
)= 40.  E= 50.
ATA POINTS=  7

BL= 0.688901  B= 0.736745  BH= 0.784588
OISL=0.230077  POIS=0.252018  POISH=0.271141
)= 50.  E= 60.
ATA POINTS=  4
```

```
= 0.661402   B= 0.823560   BH= 0.[illegible]
ISL=0.215950   POIS=0.284980   POISH=0.330109
300.   E=310.
TA POINTS=   4

= 0.647251   B= 0.714792   BH= 0.782333
ISL=0.208189   POIS=0.242336   POISH=0.270296
340.   E=350.
TA POINTS=   5


A=DM   LAT= 34.1075   LONG=106.8079
= 0.698513   B= 0.774222   BH= 0.849931
ISL=0.234740   POIS=0.267210   POISH=0.293579
250.   E=260.
TA POINTS=   5


A=SC   LAT= 34.0100   LONG=107.0894
= 0.551911   B= 0.831333   BH= 1.111754
ISL=0.144994   POIS=0.287741   POISH=0.355471
 30.   E= 40.
TA POINTS=   3

= 0.752153   B= 0.801715   BH= 0.851271
ISL=0.258460   POIS=0.277399   POISH=0.294001
 40.   E= 50.
TA POINTS=   7

= 0.688901   B= 0.736745   BH= 0.784588
ISL=0.230077   POIS=0.252018   POISH=0.271141
 50.   E= 60.
TA POINTS=   4

= 0.743411   B= 0.766561   BH= 0.787711
ISL=0.254839   POIS=0.264233   POISH=0.273043
 60.   E= 70.
TA POINTS=  18

= 0.820264   B= 0.844294   BH= 0.868325
ISL=0.283864   POIS=0.291790   POISH=0.299248
 70.   E= 80.
TA POINTS=   3

= 0.778804   B= 0.796109   BH= 0.813415
ISL=0.268962   POIS=0.275383   POISH=0.281513
 80.   E= 90.
TA POINTS=   3

= 0.665936   B= 0.773851   BH= 0.881766
ISL=0.218364   POIS=0.267067   POISH=0.308230
 90.   E=100.
TA POINTS=   3


A=WT   LAT= 34.0722   LONG=106.9459
= 0.712021   B= 0.772080   BH= 0.832139
ISL=0.241068   POIS=0.266384   POISH=0.287842
 50.   E= 60.
TA POINTS=   7

= 0.712256   B= 0.810803   BH= 0.909351
ISL=0.241176   POIS=0.280606   POISH=0.311008
 60.   E= 70.
TA POINTS=   5

= 0.657139   B= 0.753867   BH= 0.850596
ISL=0.213649   POIS=0.259158   POISH=0.293789
200.   E=210.
TA POINTS=   4

= 0.641023   B= 0.795740   BH= 0.950457
ISL=0.204658   POIS=0.275249   POISH=0.321701
210.   E=220.
TA POINTS=   3

= 0.595871   B= 0.725950   BH= 0.856029
ISL=0.176753   POIS=0.247334   POISH=0.295488
230.   E=240.
TA POINTS=   4

= 0.643194   B= 0.738140   BH= 0.833086
ISL=0.205857   POIS=0.252613   POISH=0.288154
240.   E=250.
TA POINTS=   7

= 0.693914   B= 0.761530   BH= 0.829147
ISL=0.232526   POIS=0.262243   POISH=0.286351
250.   E=260.
TA POINTS=   7

= 0.731410   B= 0.827523   BH= 0.923636
ISL=0.241722   POIS=0.286310   POISH=0.314840
260.   E=270.
TA POINTS=   8
```

STOP 0 00:00:22

Socorro Raypath Analysis Using Forced Wadati Origin Times

STA=SL LAT= 34.2000 LONG=106.0000
BL= 0.686081 B= 0.736424 BH= 0.786767
POISL=0.228683 POIS=0.245481 POISH=0.262279
D=190. E=200.
DATA POINTS= 3

STA=FR LAT= 34.0000 LONG=106.0000

STA=BG LAT= 34.2068 LONG=106.8205

STA=CU LAT= 34.1573 LONG=106.7785

STA=TA LAT= 34.0498 LONG=106.7751
BL= 0.656961 B= 0.718735 BH= 0.780508
POISL=0.218552 POIS=0.244121 POISH=0.269607
D=340. E=350.
DATA POINTS= 3

STA=OM LAT= 34.1075 LONG=106.8079
BL= 0.734051 B= 0.764537 BH= 0.795023
POISL=0.250363 POIS=0.263436 POISH=0.274988
D=240. E=250.
DATA POINTS= 3

BL= 0.743627 B= 0.748332 BH= 0.754138
POISL=0.254493 POIS=0.257115 POISH=0.259268
D=250. E=260.
DATA POINTS= 4

BL= 0.675875 B= 0.742023 BH= 0.809971
POISL=0.223536 POIS=0.254635 POISH=0.280316
D=350. E=360.
DATA POINTS= 3

STA=FM LAT= 34.0829 LONG=106.8040
BL= 0.745719 B= 0.775236 BH= 0.804953
POISL=0.255303 POIS=0.267638 POISH=0.278551
D=210. E=220.
DATA POINTS= 3

BL= 0.740336 B= 0.767626 BH= 0.794917
POISL=0.253543 POIS=0.264651 POISH=0.274949
D=250. E=260.
DATA POINTS= 7

BL= 0.733349 B= 0.754863 BH= 0.776377
POISL=0.250561 POIS=0.259562 POISH=0.268036
D=260. E=270.
DATA POINTS= 5

BL= 0.725467 B= 0.757938 BH= 0.790409
POISL=0.247121 POIS=0.260305 POISH=0.273301
D=270. E=280.
DATA POINTS= 6

STA=IC LAT= 34.0000 LONG=106.0000
BL= 0.685850 B= 0.718429 BH= 0.751007
POISL=0.228569 POIS=0.243983 POISH=0.257989
D= 20. E= 30.
DATA POINTS= 3

BL= 0.704936 B= 0.755740 BH= 0.806494
POISL=0.237805 POIS=0.259918 POISH=0.279095
D=310. E=320.
DATA POINTS= 5

BL= 0.632468 B= 0.724262 BH= 0.816053
POISL=0.199669 POIS=0.246539 POISH=0.282425
D=330. E=340.
DATA POINTS= 3

BL= 0.737417 B= 0.771156 BH= 0.805376
POISL=0.252335 POIS=0.266119 POISH=0.278731
D=350. E=360.
DATA POINTS= 3

= 0.[illegible] B= [illegible] BH= [illegible]
ISL=0.[illegible] POIS=1.[illegible] POISH=0.[illegible]
210. E=220.
TA POINTS= 3

= 0.740336 B= 0.757626 BH= 0.794917
ISL=0.253543 POIS=0.264451 POISH=0.274949
250. E=260.
TA POINTS= 7

= 0.733349 B= 0.754863 BH= 0.776377
ISL=0.250561 POIS=0.259567 POISH=0.268036
260. E=270.
TA POINTS= 5

= 0.726467 B= 0.757938 BH= 0.799409
ISL=0.247121 POIS=0.260905 POISH=0.273301
270. E=280.
TA POINTS= 6

A=IC LAT= 34.0000 LONG=106.0000
= 0.695850 B= 0.718429 BH= 0.751007
ISL=0.228569 POIS=0.243983 POISH=0.257989
20. E= 30.
TA POINTS= 3

= 0.704936 B= 0.755740 BH= 0.806494
ISL=0.237805 POIS=0.259918 POISH=0.279095
310. E=320.
TA POINTS= 5

= 0.632468 B= 0.724263 BH= 0.816058
ISL=0.199690 POIS=0.246539 POISH=0.282425
330. E=340.
TA POINTS= 3

= 0.737417 B= 0.771396 BH= 0.805376
ISL=0.252305 POIS=0.266119 POISH=0.278701
350. E=360.
TA POINTS= 6

A=WW LAT= 34.0000 LONG=106.0000
= 0.748082 B= 0.788291 BH= 0.823499
ISL=0.256785 POIS=0.272518 POISH=0.286635
290. E=300.
TA POINTS= 5

= 0.705938 B= 0.718274 BH= 0.733610
ISL=0.238250 POIS=0.243913 POISH=0.249375
340. E=350.
TA POINTS= 5

A=CC LAT= 34.1442 LONG=106.9812
= 0.743824 B= 0.758078 BH= 0.772332
ISL=0.255013 POIS=0.260861 POISH=0.266482
130. E=140.
TA POINTS= 3

= 0.723720 B= 0.740617 BH= 0.757514
ISL=0.246349 POIS=0.253664 POISH=0.260634
140. E=150.
TA POINTS= 8

= 0.723109 B= 0.739324 BH= 0.755539
ISL=0.246077 POIS=0.253116 POISH=0.259837
170. E=180.
TA POINTS= 7

= 0.711492 B= 0.756968 BH= 0.802445
ISL=0.240826 POIS=0.260414 POISH=0.277660
130. E=190.
TA POINTS= 3

= 0.717292 B= 0.746385 BH= 0.775477
ISL=0.243470 POIS=0.256031 POISH=0.267693
190. E=200.
TA POINTS= 7

= 0.722281 B= 0.759348 BH= 0.796415
ISL=0.244815 POIS=0.260970 POISH=0.275493
200. E=210.
TA POINTS= 6

= 0.722884 B= 0.747902 BH= 0.772920
ISL=0.245977 POIS=0.256710 POISH=0.266709
210. E=220.
TA POINTS= 7

TA=SC LAT= 34.0100 LONG=107.0894
L= 0.737024 B= 0.758717 BH= 0.780410
ISL=0.252133 POIS=0.261118 POISH=0.269573
= 30. E= 40.
ATA POINTS= 4

= 0.[illegible] B= [illegible] BH= [illegible]

DATA POINTS= 7

STA=SC LAT= 34.0100 LONG=107.0894
BL= 0.737024 B= 0.758717 BH= 0.780410
POISL=0.252133 POIS=0.261118 POISH=0.269570
D= 30. E= 40.
DATA POINTS= 4

BL= 0.745722 B= 0.783244 BH= 0.820767
POISL=0.255805 POIS=0.270618 POISH=0.284035
D= 40. E= 50.
DATA POINTS= 5

BL= 0.726925 B= 0.747796 BH= 0.768667
POISL=0.247763 POIS=0.256666 POISH=0.265057
D= 50. E= 60.
DATA POINTS= 5

BL= 0.743557 B= 0.754279 BH= 0.765000
POISL=0.254300 POIS=0.259325 POISH=0.263619
D= 60. E= 70.
DATA POINTS= 17

BL= 0.767172 B= 0.785987 BH= 0.804802
POISL=0.264473 POIS=0.271663 POISH=0.278497
D= 70. E= 80.
DATA POINTS= 3

BL= 0.677683 B= 0.724687 BH= 0.771691
POISL=0.224460 POIS=0.246777 POISH=0.266233
D= 80. E= 90.
DATA POINTS= 3

BL= 0.678825 B= 0.712358 BH= 0.745890
POISL=0.225041 POIS=0.241223 POISH=0.255975
D=100. E=110.
DATA POINTS= 3

STA=CM LAT= 33.9501 LONG=106.9579
BL= 0.739289 B= 0.778160 BH= 0.817348
POISL=0.253101 POIS=0.268720 POISH=0.282765
D= 0. E= 10.
DATA POINTS= 4

BL= 0.746243 B= 0.764511 BH= 0.782779
POISL=0.256022 POIS=0.263425 POISH=0.270463
D= 10. E= 20.
DATA POINTS= 10

BL= 0.751749 B= 0.771161 BH= 0.790574
POISL=0.258293 POIS=0.266028 POISH=0.273361
D=310. E=320.
DATA POINTS= 9

BL= 0.724715 B= 0.832244 BH= 0.939773
POISL=0.246789 POIS=0.287876 POISH=0.319019
D=320. E=330.
DATA POINTS= 5

BL= 0.742931 B= 0.787043 BH= 0.831155
POISL=0.254638 POIS=0.272056 POISH=0.287517
D=330. E=340.
DATA POINTS= 3

BL= 0.754878 B= 0.768219 BH= 0.781560
POISL=0.259568 POIS=0.264882 POISH=0.270004
D=340. E=350.
DATA POINTS= 10

BL= 0.723742 B= 0.768818 BH= 0.813895
POISL=0.246358 POIS=0.265117 POISH=0.281680
D=350. E=360.
DATA POINTS= 4

STA=WT LAT= 34.0722 LONG=106.9459
BL= 0.822499 B= 0.843003 BH= 0.863507
POISL=0.284622 POIS=0.291376 POISH=0.297788
D= 20. E= 30.
DATA POINTS= 3

BL= 0.734821 B= 0.765960 BH= 0.797099
POISL=0.251194 POIS=0.263977 POISH=0.275741
D= 50. E= 60.
DATA POINTS= 6

BL= 0.758233 B= 0.807769 BH= 0.857305
POISL=0.260923 POIS=0.279544 POISH=0.295883
D= 60. E= 70.
DATA POINTS= 3

BL= 0.672967 B= 0.757295 BH= 0.841623
POISL=0.222039 POIS=0.260546 POISH=0.290932
D= 70. E= 80.
DATA POINTS= 4

BL= 0.673192 B= 0.751572 BH= 0.829952

```
= 0.751749  A= 0.771161  BH= 0.793574
ISL=0.258293  POIS=0.266028  POISH=0.273361
310.  E=320.
TA POINTS=  9


= 0.724715  B= 0.832244  BH= 0.939773
ISL=0.246789  POIS=0.287876  POISH=0.329019
320.  E=330.
TA POINTS=  5


= 0.742931  B= 0.787043  BH= 0.831155
ISL=0.254633  POIS=0.272056  POISH=0.287517
330.  E=340.
TA POINTS=  3


= 0.754878  B= 0.768218  BH= 0.781560
ISL=0.259568  POIS=0.264882  POISH=0.270004
340.  E=350.
TA POINTS= 10


= 0.723742  B= 0.768818  BH= 0.813895
ISL=0.246358  POIS=0.265117  POISH=0.281680
350.  E=360.
TA POINTS=  4



A=WT  LAT= 34.0722  LONG=106.9459
= 0.822499  B= 0.843003  BH= 0.863507
ISL=0.284622  POIS=0.291376  POISH=0.297788
 20.  E= 30.
TA POINTS=  3


= 0.734821  B= 0.765960  BH= 0.797099
ISL=0.251194  POIS=0.263997  POISH=0.275741
 50.  E= 60.
TA POINTS=  6


= 0.758233  B= 0.807769  BH= 0.857305
ISL=0.260923  POIS=0.279544  POISH=0.295983
 60.  E= 70.
TA POINTS=  3


= 0.672967  B= 0.757295  BH= 0.841623
ISL=0.222039  POIS=0.260546  POISH=0.290932
 70.  E= 80.
TA POINTS=  4


= 0.673192  B= 0.751572  BH= 0.829952
ISL=0.222166  POIS=0.258221  POISH=0.287118
190.  E=200.
TA POINTS=  3


= 0.624328  B= 0.700856  BH= 0.777463
ISL=0.194832  POIS=0.238875  POISH=0.268451
200.  E=210.
TA POINTS=  3


= 0.691652  B= 0.713540  BH= 0.735429
ISL=0.231425  POIS=0.241765  POISH=0.251455
230.  E=240.
TA POINTS=  5


= 0.702666  B= 0.738646  BH= 0.774625
ISL=0.236713  POIS=0.252829  POISH=0.267365
240.  E=250.
TA POINTS=  7


= 0.736123  B= 0.756256  BH= 0.776392
ISL=0.251751  POIS=0.260126  POISH=0.268042
250.  E=260.
TA POINTS=  9


= 0.698437  B= 0.712492  BH= 0.726547
ISL=0.234704  POIS=0.241285  POISH=0.247597
260.  E=270.
TA POINTS=  5


STOP      0                                                    00:00:18
```

Bibliography

Alexandrov, K.S. and Ryzhova, T.V. (1961a). Elastic Properties of Rock-Forming Minerals, 2, Layered Silicates, Acad. Sci. USSR Bull., Geophys. Series, 11, 871-875.

Alexandrov, K.S. and Ryzhova, T.V. (1961b). Elastic Properties of Rock-Forming Minerals, 1, Pyroxenes and Amphiboles, Acad. Sci. USSR Bull., Geophys. Series, 9, 1165-1168.

Budding, A.J. (1976). Personal Communication, New Mexico Institute of Mining and Technology, Socorro, New Mexico.

Chapin, C.E. (1971). Rio Grande Rift, Part 1, Modifications and Additions, New Mexico Geol. Soc. Guidebook, 22nd Field Conf., 59-71.

Chapin, C.E. and Seager, W.R. (1975). Evolution of the Rio Grande Rift in the Socorro and Las Cruces Areas, New Mexico Geol. Soc. Guidebook, 26th Field Conf., 297-321.

Christiansen, N.I. and Fountain, D.M. (1975). Constitution of the Lower Continental Crust Based on Experimental Studies of Seismic Velocities in Granulites, Geol. Soc. Amer. Bull. 86, 227-236.

Clark, S.P., Ed. (1966). Handbook of Physical Constants, GSA Memoir 97.

Crosson, R.S. and Christiansen, N.I. (1967). Compositions of the Earth's Crust and Upper Mantle from Poisson's Ratio, Amer. Geoph. Union Trans., 48, 200.

Fagerne, V. and Kanestrom, R. (1973). Variations in the Upper Mantle Structure as Derived from Pn and Sn Waves, Pure and Applied Geophysics, 109, 1762-1772.

Hall, T. (1963). Springs in the Vicinity of Socorro, New Mexico, New Mexico Geol. Soc. Guidebook, 14th Field Conf., 160-169.

Hamilton, R.M. and Muffler, L.P. (1972). Microearthquakes at the Geysers Geothermal Area, Calif., Journ. Geoph. Research, 77, 2081-2086.

Holmes, C.R. (1963). Tritium Studies of Socorro Spring, New Mexico Geological Society Guidebook, 14th Field Conf., 152-155.

Hughes, D.S. and Maurette, C. (1956). Variation of Elastic Wave Velocities in Granites with Pressure and Temperatures, Geophysics, 21, 277-284.

Hughes, D.S. and Maurette, C. (1957). Variation of Elastic Wave Velocities in Basic Igneous Rocks with Pressure and Temperature, Geophysics, 22, 23-31.

Kisslinger, C. and Engdahl, E.R. (1973). The Interpretation of the Wadati Diagram with Relaxed Assumptions, Bull. Seis. Soc. Amer., 63, 1723-1736.

Korde, H. and Bhattacharji, S. (1975). Formation of Fractures Around Magmatic Intrusions and Their Role in Ore Localization, Economic Geology, 70, 781-799.

Lange, A.L. and Westphal, W.H. (1969). Microearthquakes Near the Geysers, Sonoma County, Calif., Journ. Geoph. Res., 74, 4377-4378.

McNitt, J.R. (1963). Exploration and Development of Geothermal Power in Calif., Calif. Division of Mines and Geology, Spec. Report 75, 45p.

Mott, R.P. (1976). The Relationship of Microearthquake Activity to Structural Geology for the Region Around Socorro, New Mexico, M.S. Ind. Study, Geos. Dept., New Mexico Inst. Mining and Tech., 64p.

Muffler, L.P. and Williams, D.L. (1976). Geothermal Investigation of the U.S.G.S. in Long Valley, Calif., 1972-73, Journ. Geoph. Research, 81, 721-724.

Nur, A. and Simmons, G. (1969). The Effect of Saturation on Velocity in Low Porosity Rocks, Earth and Planetary Science Letters, 7, 183-193.

Rinehart, E. (1976). The Use of Microearthquakes to Map an Extensive Magma Body in the Socorro, N.M., Area, M.S. Ind. Study, Geos. Dept., New Mexico Inst. Mining and Tech., p.

Sakdejayont, K. (1974). A Study of Poisson's Ratio in the Rio Grande Rift, New Mexico, M.S. Ind. Study, New Mexico Inst. Mining Tech., 28p.

Sanford A. and Reiter, M. (1976). Paper in Preparation.

Shimozuru, D. (1963). Geophysical Evidences for Suggesting the Existence of Molten Pockets in the Earth's Upper Mantle, Bull. Volc., Tome 26, 181-193.

Shuleski, P. (1976). Seismic Fault Motion and SV Wave Screening by Shallow Magma Bodies in the Vicinity of Socorro, New Mexico, M.S. Ind. Study Geos. Dept., New Mexico Inst. Mining and Tech., 94p.

Solomon, S.C. (1973). Shear Wave Attenuation and Melting Beneath the Mid-Atlantic Ridge, Journ. Geoph. Res., 78, 6044-6059.

Toppozada, T.R. (1974). Seismic Investigation of Crustal Structure and Upper Mantle Velocity in the State of New Mexico and Vicinity, Ph.D. Dissertation, New Mexico Institute of Mining and Tech., 152p.

Toppozada, T.R. and Sanford A.R. (1976). Crustal Structure in Central New Mexico, interpreted from the Gasbuggy Explosion, Bull. Seism. Soc. Amer., 66, 877-886.

Walsh, J.B. (1969). New Analysis of Attenuation in Partially Melted Rock, Journ. Geoph. Res., 74, 4333-4337.

Ward, P.L. and Bjornsson, S. (1971). Microearthquakes,

Swarms, and the Geothermal Areas of Iceland, Journ. Geoph. Res., 76, 3953-3982.

Seismicity Report on Black Rock Desert Project Northwest Nevada, (1974). Micro Geophysics Corporation.

Seismicity Report on the Adak Island Project, Aleutian Islands, Alaska, (1975). Micro Geophysics Corporation.